Research Article

Multi-Scale Temporal Resonance Theory of Consciousness (MSTRT): From Molecular Mechanisms to Minimal Functional Specifications, Necessary and Sufficient Conditions, and the Role of Sensory Input, Memory, and Motivational Drive

Yat Ho TIU[1]

1. Independent researcher

The Multi-Scale Temporal Resonance Theory (MSTRT) proposes that the physical basis of consciousness lies in nonlinear nested coupling (Phase-Amplitude Coupling, PAC) among neural oscillations at multiple temporal scales. This coupling must span a sufficiently broad frequency range, a sufficiently large spatial extent, and must exhibit a specific causal directionality (top-down dominance). The foundational cellular mechanism is backpropagation-activated calcium (BAC) firing in layer 5 thick-tufted pyramidal neurons, whose intrinsic ion channel kinetics naturally produce theta-gamma nesting; this mechanism is regulated by an inhibitory interneuron triad (SST/PV/VIP) that implements competitive selection and attentional gating, and modulated by neuromodulatory systems acting as a unified gain control parameter. This paper presents the complete architecture of MSTRT across three planes: (i) a deep biophysical analysis of consciousness-critical structures from the molecular level, including the formal mathematical link from single-neuron BAC firing statistics to population-level PAC; (ii) a computable mathematical framework comprising a structural index (Functional Resonance Potential, FRP), a dynamic index (Extended Dynamic Resonance Realization, EDRR), and a composite consciousness index ($CSDI_{2.0}$); and (iii) six substrate-independent Minimal Functional Specifications (MFS) distilled from rigorous substitutability analysis.

 doi.org/10.32388/YKIRJL

The paper further introduces a detailed empirical and philosophical analysis of three domains frequently assumed to be necessary for consciousness: sensory input, memory, and motivational drives. Drawing on evidence from sensory deprivation, dreaming, clinical amnesia, contemplative neuroscience, hydranencephaly, locked-in syndrome, blindsight, akinetic mutism, and interoceptive inference, we evaluate whether each domain constitutes a necessary condition for consciousness or merely a content source that shapes what consciousness is about. We find that external sensory input is clearly not necessary; that long-term memory is not necessary but ultra-short-term temporal buffering (on the order of one theta cycle, ~200–250 ms) likely is; and that motivational drive is so deeply entangled with the biological arousal systems enabling consciousness that separating the two may be practically impossible in any naturally occurring system, even though the entanglement may not reflect a logical or metaphysical necessity. These findings refine the MSTRT framework by making explicit what its architecture already implicitly contains: temporal buffering is embedded in MFS-1 and MFS-2, and drive-linked arousal is embedded in MFS-5.

The paper integrates MSTRT with major existing theories (IIT, GWT, HOT, DIT, predictive coding), articulates its philosophical position of Process Structuralism, and proposes seven falsifiable experimental predictions. Implications for artificial consciousness, clinical disorders of consciousness, cross-species comparison, and the philosophical question of whether consciousness can exist without purpose are discussed.

Corresponding author: Y.H. TIU, tiuyatho@gmail.com

Chapter 1: Introduction

1.1. The Problem

Consciousness remains one of the deepest unsolved problems in the natural sciences. Despite three decades of remarkable progress in neuroscience, we still lack a unified theoretical framework capable of answering, from first physical principles, a set of core questions: Why are specific brain structures indispensable for consciousness? What is biophysically unique about those structures at the molecular level? Could a system simpler than the human brain give rise to some form of consciousness, and if so, what are the minimum requirements?

The leading theories of consciousness each offer important insights but also carry significant limitations. Tononi's Integrated Information Theory (IIT) posits that consciousness equals integrated information, denoted Φ, and provides a rigorous mathematical formulation. However, computing Φ for real brains is an NP-hard problem whose computational complexity scales exponentially with system size, rendering it practically intractable[1]. Baars' and Dehaene's Global Workspace Theory (GWT) accurately describes the functional process by which information is "broadcast" to a global workspace, but does not specify the physical mechanism or triggering conditions for this broadcast[2][3]. Rosenthal's Higher-Order Theory (HOT) argues philosophically for the necessity of higher-order representations, but lacks a concrete neurobiological implementation plan. More recently, Aru, Suzuki, and Larkum[4] proposed the Dendritic Integration Theory (DIT), which identifies apical dendritic activity in Layer 5 pyramidal neurons as a cellular-level mechanism of consciousness. DIT provides a crucial cellular foundation, but does not extend into a complete multi-scale dynamical systems framework with computable indices and substrate-independent minimal specifications.

This paper introduces the **Multi-Scale Temporal Resonance Theory (MSTRT)**, which attempts to bridge the gaps among the theories above and provide a quantifiable, testable, and operationally complete framework. MSTRT builds upon and significantly extends DIT's cellular insight by embedding it within a multi-scale oscillatory dynamics framework equipped with computable indices and minimal functional specifications. The central thesis of MSTRT is: **The physical basis of consciousness lies in nonlinear nested coupling (Phase-Amplitude Coupling, PAC) among neural oscillations at multiple temporal scales. This coupling must span a sufficiently broad frequency range, a sufficiently large spatial extent, and must exhibit a specific causal directionality (top-down dominance).**

1.2. The Problem of Necessary Conditions

Beyond the question of mechanism, consciousness science has been less systematic in distinguishing necessary conditions (without which consciousness cannot exist) from contingent content sources (which shape conscious experience but whose absence does not extinguish it). This distinction matters profoundly for theory construction: a theory that treats a content source as a necessary condition will make incorrect predictions about when consciousness is present or absent, with direct consequences for clinical assessment (e.g., disorders of consciousness), ethical judgment (e.g., animal and fetal consciousness), and engineering (e.g., artificial consciousness).

This paper extends the mechanistic account of MSTRT by systematically examining three domains that are commonly assumed, explicitly or implicitly, to be necessary for consciousness: sensory input from the external world, memory (in its multiple forms), and motivational drives or desires. Together, these three domains span the three temporal orientations of consciousness: sensory input grounds consciousness in the present (what is happening now), memory connects consciousness to the past (what has happened before), and motivational drive orients consciousness toward the future (what the organism needs or wants to happen next). If all three were necessary, consciousness would require simultaneous engagement with past, present, and future — a strong architectural constraint. If none were necessary in their full form, consciousness would be a far more minimal phenomenon than ordinarily assumed, reducible to a bare mechanism that can operate on any content or none at all.

1.3. Paper Structure

This paper comprises nine chapters. Chapter 1 is the present introduction. Chapter 2 provides an in-depth biophysical analysis of the molecular foundations of consciousness-critical structures, including a treatment of inhibitory interneuron gating, the formal link between BAC firing statistics and PAC strength, and a general framework for neuromodulatory gain control. Chapter 3 establishes the complete mathematical framework, including the structural index (FRP), the dynamic index (EDRR), and the composite consciousness index ($CSDI_{2.0}$). Chapter 4 conducts a rigorous analysis of structural necessity, including an expanded treatment of the "temporal grain" hypothesis. Chapter 5 distills the Minimal Functional Specifications (MFS) and explores the possibility of simplified structures. Chapter 6 presents the detailed empirical evaluation of sensory input, memory, and motivational drive as candidate necessary conditions for consciousness, and synthesizes the findings. Chapter 7 integrates and compares MSTRT with other major theories of consciousness. Chapter 8 proposes testable experimental predictions. Chapter 9 provides discussion and conclusions.

1.4. Methodological Statement

The methodology of this research operates on three planes. At the **empirical plane**, it synthesizes published research in neuroscience, biophysics, clinical medicine, and contemplative neuroscience, with particular emphasis on studies of anesthesia, sleep, brain injury, drug effects, sensory deprivation, amnesia, and meditative states. At the **theoretical plane**, it employs deductive reasoning from cable theory, ion channel kinetics, coupled oscillator theory, information theory, and evolutionary neurobiology. At the **mathematical plane**, it constructs quantifiable indices and computable models.

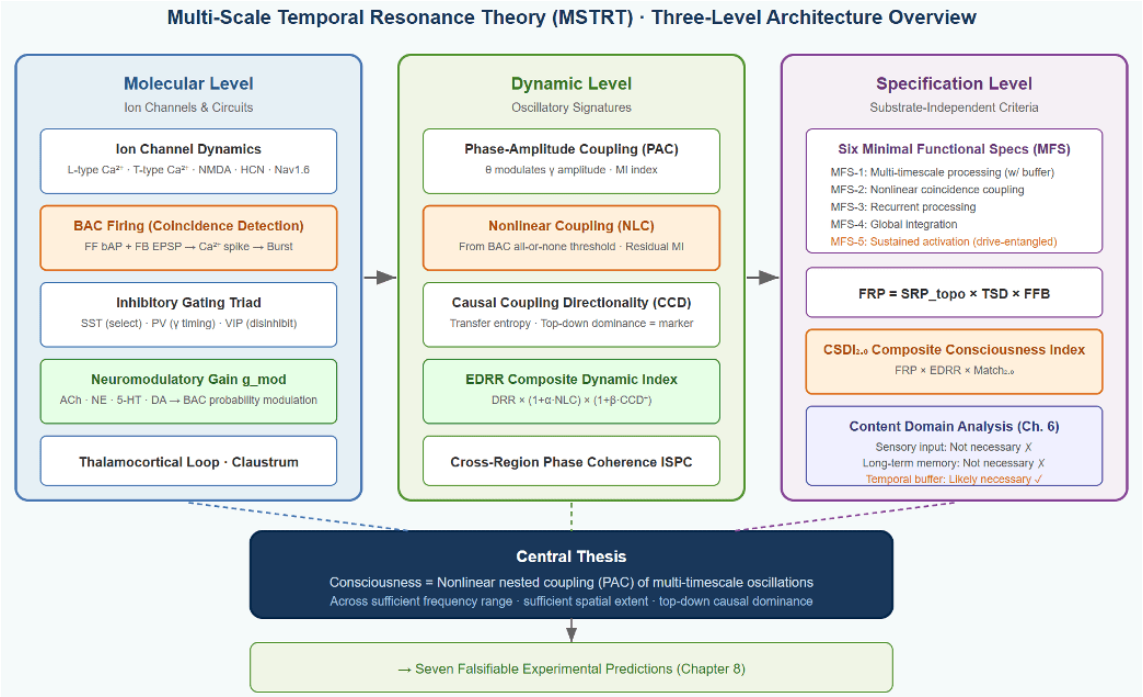

Figure 1. Overview of the Multi-Scale Temporal Resonance Theory (MSTRT). The theory operates across three levels. The **Molecular Level** (left) identifies the specific ion channels (L-type Ca^{2+}, T-type Ca^{2+}, NMDA, HCN, Nav1.6) and circuits (BAC firing mechanism, SST/PV/VIP inhibitory gating triad, thalamocortical loop) that generate the critical temporal dynamics underlying consciousness, along with the neuromodulatory gain parameter g_{mod} that controls BAC firing probability. The **Dynamic Level** (center) formalizes the emergent oscillatory signatures — phase-amplitude coupling (PAC/MI), nonlinear coupling strength (NLC), and causal coupling directionality (CCD) — into the computable Extended Dynamic Resonance Realization index (EDRR). The **Specification Level** (right) distills six substrate-independent Minimal Functional Specifications (MFS-1 through MFS-6) and integrates all metrics into the composite consciousness index $CSDI_{2.0}$ = FRP × EDRR × $Match_{2.0}$. All three levels converge on the central thesis (bottom dark blue box): consciousness requires nonlinear nested coupling of multi-timescale oscillations. Analysis of sensory input, memory, and motivational drive (Chapter 6, lower-right blue box) establishes which domains are content sources rather than necessary conditions, further refining the specification level. Dashed arrows indicate each level's contribution to the central thesis.

Relationship to Prior Work: Dendritic Integration Theory and Apical Amplification. It is essential to acknowledge that the molecular-level foundation of MSTRT is not novel in isolation, but builds directly and substantially upon the Dendritic Integration Theory (DIT) of Aru, Suzuki, and Larkum[4] and the broader apical amplification (AA) framework developed by Phillips, Larkum, Bachmann, and Storm over

doi.org/10.32388/YKIRJL

the past two decades[5] (Larkum, Senn, & Lüscher, 2004; Phillips, 2017; Phillips, Bachmann, & Storm, 2018; Bachmann & Hudetz, 2014). The BAC firing mechanism, the dual-compartment integration architecture of Layer 5 pyramidal neurons, the role of apical dendrites as a locus for feedback integration, the identification of burst firing as a signal of feedforward-feedback coincidence, and the account of how general anesthetics abolish consciousness by disrupting apical function — all of these insights originate from, or were substantially anticipated by, the DIT/AA research program. What MSTRT seeks to contribute beyond this foundation is threefold: first, an explicit mechanistic argument that the BAC firing cycle intrinsically generates θ-γ phase-amplitude coupling at the single-neuron level (burst duration → γ, AHP refractory period → θ), thereby grounding a network-level oscillatory signature in cellular biophysics; second, a computable mathematical framework ($CSDI_{2.0}$ = FRP × EDRR × $Match_{2.0}$) that formalizes the relationship between structural connectivity, dynamic oscillatory realization, and their alignment into a single quantitative index; and third, a set of substrate-independent minimal functional specifications (MFS-1 through MFS-6) and a concrete three-layer minimal conscious system architecture designed to be testable via computational simulation. MSTRT should therefore be understood not as a replacement for DIT/AA, but as an attempt to extend and formalize those insights into a broader, multi-level, and quantitatively falsifiable theoretical framework.

Chapter 2: Deep Biophysical Analysis of Consciousness-Critical Structures

2.1. Overview: Four Key Structures and Their Functional Roles

Multiple converging lines of neuroscientific evidence point to four structures as critical for consciousness: **Layer 5 pyramidal neurons (L5 PNs)**, **thalamocortical circuits**, **cortical recurrent connections**, and the **claustrum**. This chapter analyzes the molecular and biophysical properties of these structures in depth, explaining why precisely these structures—rather than others—are intimately linked to consciousness. It also addresses the critical but often overlooked role of inhibitory interneuron microcircuits in gating consciousness-related dynamics, the formal mathematical link between cellular-level BAC firing and population-level PAC, and the general role of neuromodulatory systems as gain controls on conscious processing.

2.2. Layer 5 Pyramidal Neurons — The Molecular Nexus of Consciousness

2.2.1. Morphological Features and Cable Theory Analysis

Thick-tufted Layer 5 pyramidal neurons (L5tt-PNs) are among the largest neurons in the mammalian neocortex. Their cell bodies (somata) reside in cortical Layer 5 (approximately 1.2–1.5 mm from the pial surface), while their apical dendrites extend all the way to Layer 1 (the cortical surface), spanning a total length of 1.5–2 mm. At the cellular scale, this distance is enormous—exceeding 100 times the soma diameter.

To appreciate the functional significance of this morphology, one must apply neuronal **cable theory**. A long dendrite can be modeled as a passive cable along which electrical signals attenuate exponentially. The characteristic length scale of attenuation is the **length constant** λ:

$$\lambda = \sqrt{\frac{R_m \cdot d}{4R_i}}$$

where $R_m$is the specific membrane resistance (typical value ~10,000–50,000 Ω·cm²), $d$is the dendrite diameter (typical ~2–5 μm), and $R_i$is the axoplasmic resistivity (typical ~100–200 Ω·cm).

Substituting representative values ($R_m = 20,000$ Ω·cm², $d = 3$μm, $R_i = 150$Ω·cm):

$$\lambda = \sqrt{\frac{20000 \times 3 \times 10^{-4}}{4 \times 150}} = \sqrt{\frac{6}{600}} = \sqrt{0.01} = 0.1 \text{ cm} = 1000\ \mu\text{m}$$

In practice, however, owing to progressive tapering and branching of the apical dendrite, the effective length constant is considerably shorter—approximately 200–400 μm (Rall, 1967; Stuart & Spruston, 1998).

A passive electrical signal generated at the top of the apical dendrite (Layer 1) and traveling to the soma (Layer 5, a distance $d \approx 1500$μm) would attenuate as:

$$V_{\text{soma}} = V_{\text{tuft}} \cdot e^{-d/\lambda}$$

Taking a conservative $\lambda = 300$μm:

$$V_{\text{soma}} = V_{\text{tuft}} \cdot e^{-1500/300} = V_{\text{tuft}} \cdot e^{-5} \approx V_{\text{tuft}} \times 0.0067$$

This represents attenuation exceeding 99.3%. A 10 mV excitatory postsynaptic potential (EPSP) at the apical tuft would arrive at the soma as a mere ~0.07 mV—entirely buried in membrane potential noise (~0.5–1 mV rms).

Core inference: Purely passive electrotonic conduction cannot effectively transmit apical dendritic signals to the soma. For distal synaptic inputs to influence neuronal output, an active signal amplification mechanism is required.

2.2.2. Active Dendrites — Precision Deployment of Ion Channels

Evolution's solution to the above physical constraint is to deploy **active ion channels** along the apical dendrite—transforming it from a passive cable into an active cable capable of generating regenerative electrical signals (dendritic spikes).

The following describes the distribution of critical ion channels from apex to base:

(i) Apical dendritic tuft (Layer 1): High density of **L-type calcium channels** (CaV1.2 and CaV1.3; encoded by the CACNA1C and CACNA1D genes, respectively). L-type calcium channels have an activation threshold of approximately -40 mV, relatively slow activation kinetics (activation time constant ~5–20 ms), and extremely slow inactivation (hundreds of milliseconds to seconds), enabling sustained Ca^{2+} influx[6].

(ii) Upper apical trunk (Layers 2–3): Moderate density of **T-type calcium channels** (CaV3.1, encoded by CACNA1G). T-type (T = transient) channels have a lower activation threshold (~-60 mV) but inactivate rapidly (inactivation time constant ~20–50 ms). They can be activated at lower membrane potentials, functioning as first-stage signal amplifiers.

(iii) Calcium initiation zone (nexus zone at the Layer 3–4 border/main bifurcation point): This region co-expresses L-type and **R-type calcium channels** (CaV2.3, encoded by CACNA1E), along with synaptic NMDA receptors. R-type channel kinetics are intermediate between L-type and T-type. When depolarization at this zone reaches threshold, it triggers an all-or-none **dendritic calcium spike**—the core event of BAC firing. The existence of a discrete calcium initiation zone has been directly confirmed by Larkum and colleagues through dual-electrode recording and calcium imaging[7].

The HCN density gradient has dual functional significance. On one hand, it "normalizes" the influence of synapses at different locations on the soma—HCN channel opening reduces local membrane impedance, shunting proximal EPSPs and partially compensating for the distance-dependent attenuation disadvantage of distal synapses. On the other hand, HCN channels reduce the membrane time constant $\tau_m = R_m \cdot C_m$ (by effectively lowering R_m), narrowing the temporal integration window—meaning only signals that arrive nearly simultaneously can summate effectively. The cost is that individual distal

synaptic signals become even less able to influence the soma passively, making them entirely dependent on the active calcium spike mechanism to bridge the distance.

(iv) Along the entire apical trunk: HCN channels (Hyperpolarization-activated Cyclic Nucleotide-gated channels), encoded by HCN1 and HCN2 genes. HCN channels activate upon hyperpolarization (opposite to most voltage-gated channels), producing a mixed Na^+/K^+ inward current (I_h). A key feature of HCN channels is that their density **increases progressively** from soma to apex—apical density is approximately 6–10 times that at the soma[8][9].

(v) Axon hillock and axon initial segment (AIS): Very high density of **Nav1.6 sodium channels** (encoded by SCN8A). This is the site of action potential initiation. Nav1.6 has the lowest activation threshold among all sodium channel subtypes (approximately −55 mV), ensuring that action potentials are initiated here first[10].

2.2.3. The Complete Biophysical Mechanism of BAC Firing

BAC firing (Backpropagation-Activated Calcium spike firing) was first described by Matthew Larkum, Jiajun Zhu, and Bert Sakmann in 1999 in *Nature*[5]. Its complete physical process unfolds as follows:

Step 1: Feedforward input triggers an action potential. Feedforward signals from Layer 4 (thalamic relay → L4 spiny stellate → L5) arrive at the basal dendrites and perisomatic synapses of L5tt-PNs. When the input is sufficiently strong, it triggers a standard sodium action potential (Na^+ AP) at the axon initial segment. The action potential depolarizes the membrane by approximately +100 mV (from −70 mV to +30 mV) and lasts approximately 1 ms.

Step 2: The action potential backpropagates. The action potential propagates not only orthodromically along the axon but also antidromically into the apical dendrite. This is the **backpropagating action potential (bAP)**. The bAP amplitude attenuates during propagation—owing to the tapering dendrite diameter (increasing axial resistance) and shunting by HCN channels—from ~100 mV at the soma to approximately 30–50 mV at the calcium initiation zone[11]. The bAP propagation velocity is approximately 0.5–1 m/s, reaching the calcium initiation zone with a delay of approximately 1.5–3 ms.

Step 3: Coincident arrival of feedback input. Nearly simultaneously (within a ~5–30 ms time window), feedback signals from Layer 1 arrive at the apical dendritic tuft. These feedback signals originate from higher-order cortical areas via cortico-cortical feedback projections and from the thalamic intralaminar nuclei (ILN) via non-specific projections. The feedback signals produce local depolarization (EPSPs)

through postsynaptic AMPA and NMDA receptors, and this depolarization wave propagates down the apical trunk toward the calcium initiation zone.

Step 4: Coincidence triggers a calcium spike. When the bAP and the apical EPSP temporally coincide at the calcium initiation zone, their summation drives the local membrane potential past the activation threshold for L-type and R-type calcium channels (approximately -40 mV). Once the threshold is crossed, channel opening causes massive Ca^{2+} influx, further depolarizing the membrane and opening additional calcium channels—creating a positive feedback loop—that triggers a large, sustained **dendritic calcium spike** lasting tens of milliseconds. This is an **all-or-none** event: either the two signals coincide within the window, reach threshold, and trigger the full calcium spike; or they do not coincide, threshold is not reached, and nothing happens. There is no "half" calcium spike.

Step 5: The calcium spike drives burst firing. The calcium spike generates a large positive current that flows from the calcium initiation zone back to the soma. This current produces a sustained depolarizing plateau at the soma lasting approximately 50–100 ms, upon which a train of high-frequency sodium action potentials is triggered—**burst firing** at ~100–300 Hz, comprising 3–8 action potentials.

Step 6: Brain-wide broadcast of the burst signal. L5tt-PN axons project widely, including to contralateral cortex, ipsilateral distant cortical areas, thalamus (particularly higher-order relay nuclei and ILN), and multiple subcortical structures (superior colliculus, pontine nuclei, spinal cord, etc.). The burst discharge "broadcasts" an unambiguous signal across the brain: **feedforward and feedback have successfully converged at this location.**

Step 7: Refractory period and cycle reset. Following the calcium spike, the elevation in intracellular Ca^{2+} concentration activates **calcium-dependent potassium channels**—including SK channels (small-conductance calcium-activated potassium channel, KCNN gene family) and BK channels (big-conductance calcium-activated potassium channel, KCNMA1 gene)—producing a sustained **afterhyperpolarization (AHP)** lasting approximately 100–300 ms. During the AHP, the soma is hyperpolarized and resistant to new action potential generation; simultaneously, the L-type calcium channels at the initiation zone are in an inactivated state requiring time to recover. This constitutes the **refractory period** of BAC firing.

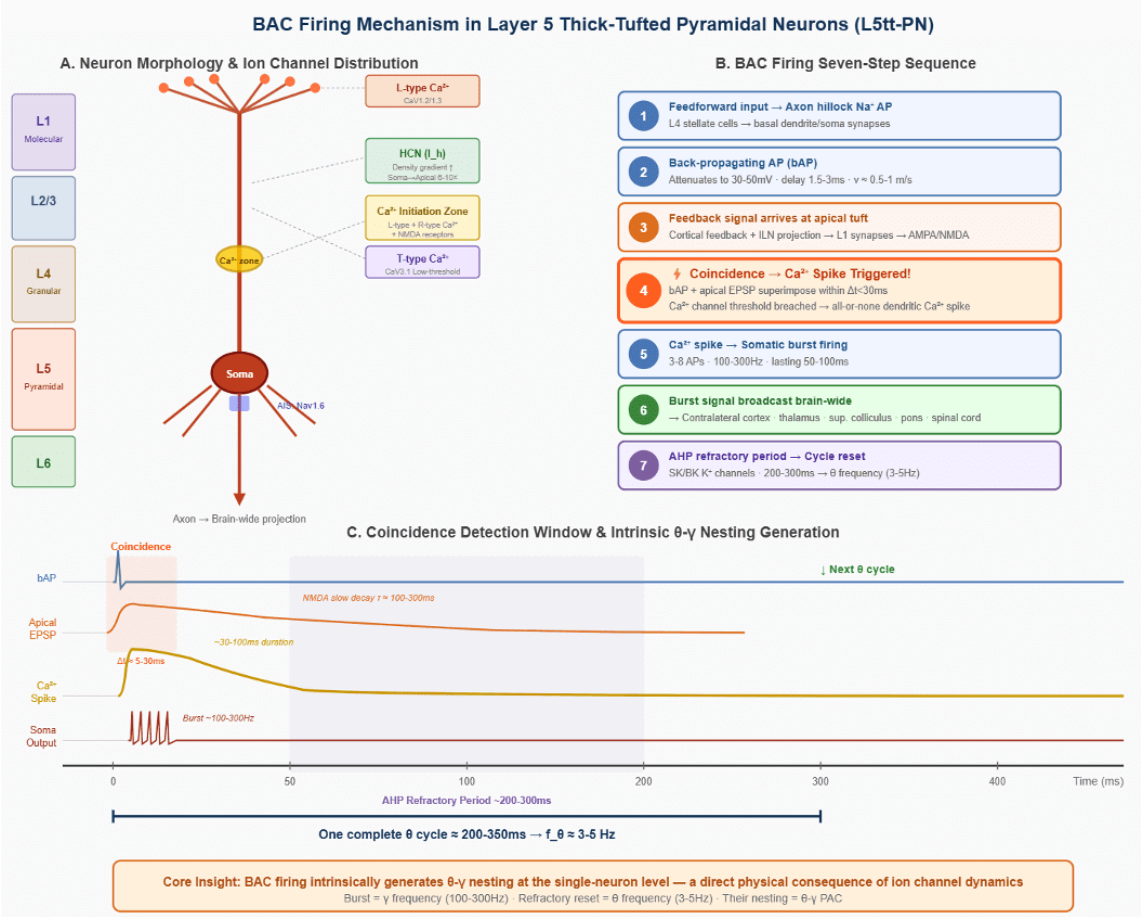

Figure 2. Complete BAC (Back-propagation Activated Calcium spike) firing mechanism in Layer 5 thick-tufted pyramidal neurons.(A) Schematic morphology of the L5tt-PN showing ion channel distribution along the apical dendrite: L-type Ca^{2+} channels (CaV1.2/1.3) at the tuft branches (Layer 1), HCN channels producing I_h current with a 6-10× density gradient increasing from soma to apex, a Ca^{2+} initiation zone (yellow ellipse) at the L3/L4 boundary co-expressing R-type Ca^{2+} channels and NMDA receptors, and Nav1.6 sodium channels at the axon initial segment (AIS). **(B)** The complete seven-step BAC firing sequence. Steps 1–2 comprise the feedforward-driven action potential and its back-propagation. Step 3 is the arrival of feedback signals at the apical tuft. The critical Step 4 (orange highlight) is coincidence detection — when the bAP and apical EPSP superimpose within a ≤30ms window to exceed the Ca^{2+} channel threshold, triggering an all-or-none regenerative dendritic calcium spike. Steps 5–6 describe the calcium spike-driven high-frequency burst firing and its brain-wide broadcast. Step 7 is the SK/BK potassium channel-mediated afterhyperpolarization (AHP) refractory period. **(C)** Detailed temporal structure of the coincidence detection window. The bAP (blue) reaches the Ca^{2+} initiation zone within ~1–3ms. The apical EPSP duration (orange) is primarily determined by NMDA receptor slow decay kinetics ($\tau \approx 100–300$ms), creating an effective coincidence window of ~5–30ms (red dashed box). Upon successful coincidence, the triggered Ca^{2+} spike (gold) lasts ~30–100ms, driving somatic high-frequency burst firing (red). The subsequent AHP refractory period (purple shaded area, ~200–

doi.org/10.32388/YKIRJL

300ms) resets the system for the next θ cycle. The bottom bracket shows that one complete BAC firing cycle corresponds to ~200–350ms, naturally producing a 3–5 Hz θ rhythm. The insight box at the bottom summarizes the core finding: θ-γ nesting is a direct physical consequence of ion channel biophysics, not an externally imposed rhythm.

2.2.4. Critical Time Constants of BAC Firing

Multiple steps of BAC firing are constrained by precise ion channel kinetics. The following time parameters derive directly from biophysical measurements of ion channels:

Duration of the bAP at the calcium initiation zone: Determined by the inactivation kinetics of dendritic sodium channels (Nav1.2, SCN2A gene). The Na^+ AP half-width is approximately 0.5–1 ms, but is broadened to approximately 1–3 ms in dendrites due to lower channel density.

Duration of the apical EPSP: Depends on synaptic receptor type. AMPA receptor-mediated EPSPs decay with a time constant of ~2–5 ms; NMDA receptor-mediated EPSPs decay with time constants of ~50–150 ms (GluN2A subtype) to ~200–300 ms (GluN2B subtype).

Effective coincidence detection window: Experimentally measured at approximately 5–30 ms[5]. This window is primarily set by the slow kinetics of NMDA receptors—the NMDA-mediated slow EPSP provides a sustained depolarization background, and the bAP need only arrive during any moment within this background to potentially trigger the calcium spike.

Duration of the calcium spike: Determined by L-type calcium channel inactivation kinetics (inactivation time constant ~50–200 ms), typically lasting approximately 30–100 ms.

AHP/refractory period duration: Determined by SK/BK potassium channel deactivation kinetics and intracellular Ca^{2+} clearance rate. SK channel deactivation time constant is ~50–150 ms; Ca^{2+} clearance time constant is ~100–500 ms (depending on the activity of endoplasmic reticulum Ca^{2+}-ATPase SERCA, plasma membrane Ca^{2+}-ATPase PMCA, and the Na^+/Ca^{2+} exchanger NCX). Total refractory period is approximately 200–300 ms.

Deep inference: A complete BAC firing cycle (trigger → calcium spike → burst firing → AHP → recovery) takes approximately 200–350 ms, corresponding to a natural cycling frequency of ~3–5 Hz—falling precisely in the **θ band (3–8 Hz)**. The burst discharge itself (~100–300 Hz) falls in the **high γ/ripple band**. This means that **the BAC firing mechanism intrinsically generates θ-γ nesting at the single-neuron**

level—precisely the core dynamical feature predicted by MSTRT. This is not a theoretical assumption but a direct physical consequence of ion channel kinetics.

2.2.5. Effects of Anesthetics on BAC Firing — A Molecular-Level Analysis

Suzuki and Larkum[12] published a landmark study in *Cell*[12] providing critical experimental evidence: general anesthetics eliminate consciousness by **specifically blocking apical dendritic calcium spikes**, while leaving the basic somatic firing capability intact. The following is a molecular-level analysis of the mechanisms of different anesthetics:

Volatile anesthetics (isoflurane, sevoflurane, etc.): Strike at BAC firing through multiple mechanisms: (i) enhancement of GABA_A receptors (subunits encoded by GABRA/GABRB genes), increasing inhibition of the apical dendrite by dendritic-targeting inhibitory interneurons; (ii) enhancement of HCN channel activity (increasing I_h current), reducing apical dendritic membrane impedance and accelerating signal decay; (iii) direct inhibition of L-type and R-type calcium channels, raising the calcium spike threshold. This triple strike simultaneously targets different stages of BAC firing.

Propofol: Primarily enhances GABA_A receptor activity (binding to the β subunit of the GABA_A receptor). Propofol has also been reported to influence HCN channels (enhancing I_h), further reducing apical dendritic impedance. Multiple studies provide supporting evidence for propofol's effects on I_h (Chen et al., 2005, J Pharmacol Exp Ther; Cacheaux et al., 2005, Mol Pharmacol), though the specific effects may vary by brain region and channel subtype.

Ketamine: As an NMDA receptor antagonist, ketamine blocks the NMDA receptor ion channel pore. The role of NMDA receptors at apical synapses is to extend the EPSP duration (from AMPA's ~5 ms to NMDA's ~50–150 ms), thereby **widening the coincidence detection window**. Blocking NMDA receptors sharply narrows this window, making BAC firing much harder to trigger. However, ketamine's pharmacology is more complex than simple NMDA blockade—it also blocks NMDA receptors on certain inhibitory interneurons, and the net effect at low doses may be **disinhibition**—a paradoxical increase in cortical excitability—which explains the dissociative/psychedelic effects of low-dose ketamine. At high doses, NMDA blockade overwhelms disinhibition, causing loss of consciousness.

Psychedelics (5-HT2A receptor agonists such as LSD, psilocybin): Psychedelics act primarily by activating **5-HT2A receptors** on the apical dendrites of L5tt-PNs[13]. 5-HT2A is a Gq protein-coupled receptor whose activation triggers the PLC-IP3-DAG signaling cascade, ultimately enhancing persistent sodium current (I_{NaP}) and reducing certain potassium channel currents. This **lowers the calcium spike**

threshold—making BAC firing easier to trigger, even when the feedback signal is weak or poorly matched to the feedforward signal. The result: more information enters the "consciousness broadcast"—but this includes large quantities of noise that would normally be filtered out by the threshold mechanism. This is consistent with subjective reports of psychedelic experience: sensory enhancement, flooding of meaning, dissolution of boundaries.

Key observation: All of the above molecular targets converge on the same physical process—**blocking or altering apical-basal signal coincidence detection**. The molecular basis of consciousness lies not in any single molecule, but in a dynamical process (BAC firing) collectively maintained by an ensemble of molecules.

2.2.6. Inhibitory Interneuron Gating of BAC Firing — The SST/PV/VIP Triad

The preceding sections describe BAC firing as a two-input coincidence detector. However, in the intact cortex, the probability and timing of BAC firing are powerfully regulated by three major classes of inhibitory interneurons, each targeting distinct compartments of the L5tt-PN and forming an interconnected microcircuit that implements competitive selection and attentional gating.

Somatostatin-positive (SST+) interneurons (Martinotti cells) preferentially target the apical dendrites of L5tt-PNs in Layers 1–3[14]. SST+ cells are recruited by local excitatory activity with a delay of approximately 10–30 ms (owing to facilitating synapses from excitatory cells onto SST+ cells). When a population of L5tt-PNs begins to fire, nearby SST+ interneurons are activated and deliver inhibition to the apical dendrites of surrounding pyramidal cells. This creates a temporal window of opportunity: only those L5tt-PNs that receive strong enough coincident input to trigger BAC firing before the SST+ inhibition arrives will successfully generate a calcium spike. Neurons with weaker or mistimed inputs are suppressed. This mechanism implements a **competitive winner-take-all selection** among nearby L5tt-PNs, ensuring that only the most "relevant" neurons—those with the best feedforward-feedback match—enter the conscious broadcast. Functionally, SST+ gating sharpens the signal-to-noise ratio of BAC firing at the population level and may underlie the limited capacity of conscious attention.

Parvalbumin-positive (PV+) interneurons provide fast perisomatic inhibition to L5tt-PNs, controlling the precise timing of somatic action potentials and thus the bAP. PV+ interneuron networks are the primary generators of cortical gamma oscillations[15]. Because PV+ inhibition gates somatic spiking at gamma frequency, the bAP is itself gamma-rhythmic—it can only be generated at specific phases of the gamma cycle when PV+ inhibition is momentarily released. This means that BAC firing is doubly gated: the bAP

must occur at a permissive gamma phase (set by PV+ cells), and the apical input must arrive within the coincidence window around that bAP. The result is that BAC firing is locked to specific gamma phases within each theta cycle, producing the phase-precise PAC that is the hallmark of conscious processing.

VIP+ (vasoactive intestinal peptide-positive) interneurons preferentially inhibit SST+ cells, creating a **disinhibition circuit**. When VIP+ cells are activated—for example, by cholinergic input from the basal forebrain during states of heightened attention, or by top-down signals from prefrontal cortex—they suppress SST+ inhibition of apical dendrites, thereby **opening the gate** for BAC firing. This VIP→SST disinhibition pathway is a likely cellular mechanism for the well-documented enhancement of conscious perception by attention. Conversely, when VIP+ activity is low (as during drowsy or inattentive states), SST+ inhibition is unopposed and BAC firing probability decreases, consistent with the dimming of consciousness.

The SST/PV/VIP triad thus adds three critical features to the BAC firing framework: competitive selection (via SST+), gamma-phase precision (via PV+), and attentional gain modulation (via VIP→SST disinhibition). These features are essential for understanding not just whether consciousness occurs, but which specific information content enters the conscious broadcast at any given moment.

2.2.7. Formal Link: From BAC Firing Statistics to PAC Strength

The preceding sections establish that individual L5tt-PNs intrinsically generate theta-gamma nesting through BAC firing. However, the measurable PAC observed in population-level recordings (EEG/ECoG/LFP) arises from the statistical properties of BAC firing across a population of neurons. This section formalizes the link.

Let the BAC firing probability per gamma cycle be $p_{\mathrm{BAC}}(\phi_\theta)$, where ϕ_θ is the current theta phase. Due to the refractory period, p_{BAC} is near zero for theta phases shortly after the previous BAC event and peaks at the phase where the refractory period has just ended and feedback input is maximal. This can be modeled as:

$$p_{\mathrm{BAC}}(\phi_\theta) = p_0 \cdot R(\phi_\theta) \cdot F(\phi_\theta) \cdot g_{\mathrm{mod}}$$

where $R(\phi_\theta) = 1 - e^{-(\phi_\theta - \phi_{\mathrm{ref}})/\tau_R}$ is the refractory recovery function (τ_R is the refractory time constant in radians of theta phase, and ϕ_{ref} is the phase of the last BAC event), $F(\phi_\theta)$ is the feedback signal strength at phase ϕ_θ (determined by the temporal profile of the theta-modulated feedback volley), and g_{mod} is the

neuromodulatory gain factor (see Section 2.9). The baseline probability $p_0$depends on the overall excitability of the neuron and the strength of feedforward input.

The expected gamma-band amplitude at theta phase $\phi_\theta$across the population is then:

$$\langle A_\gamma(\phi_\theta)\rangle = A_{\text{base}} + A_{\text{burst}} \cdot N_{\text{active}} \cdot p_{\text{BAC}}(\phi_\theta)$$

where $A_{\text{base}}$is baseline gamma amplitude from non-BAC sources (e.g., PV+ interneuron-driven gamma), A_{burst} is the gamma amplitude contribution per BAC firing event, and $N_{\text{active}}$is the number of active L5tt-PNs.

The Modulation Index (MI) used to quantify PAC is a direct function of the non-uniformity of $\langle A_\gamma(\phi_\theta)\rangle$ across theta phases. If $p_{\text{BAC}}(\phi_\theta)$is sharply peaked (narrow refractory recovery + temporally precise feedback), MI is high. If $p_{\text{BAC}}(\phi_\theta)$is broad or nearly uniform (wide recovery + temporally diffuse feedback), MI is low.

This formalization makes several important predictions explicit. First, any manipulation that broadens the refractory period distribution (e.g., pharmacological perturbation of SK channels) should reduce PAC precision and thus MI. Second, the nonlinear component of PAC (NLC, see Section 3.3.4) arises specifically from the all-or-none threshold of the calcium spike—the relationship between feedback input strength and BAC probability is a sigmoid, not a line. Third, the competitive selection by SST+ interneurons (Section 2.2.6) effectively sharpens the distribution of $p_{\text{BAC}}(\phi_\theta)$across the population by suppressing weakly driven neurons, thereby increasing population-level MI.

2.3. Thalamocortical Circuits — The Biophysical Engine of Oscillation

2.3.1. Dual Firing Modes of Thalamic Relay Neurons

Thalamic relay neurons exhibit two fundamentally distinct firing modes, governed by a unique class of ion channel—**T-type calcium channels** (CaV3.1/CACNA1G, CaV3.2/CACNA1H, CaV3.3/CACNA1I). The name "T-type" derives from the "transient" nature of their current. Their distinctive biophysical properties include: low-threshold activation (~−60 mV, far below the ~−40 mV of L-type channels), rapid inactivation (channels inactivate ~20–50 ms after opening), and a requirement for **hyperpolarization for de-inactivation** (once inactivated, the membrane potential must drop below approximately −70 mV and remain there for ~50–100 ms before the channels recover to a "primed" activatable state).

These three properties together determine two firing modes:

Tonic mode: During the waking state, brainstem arousal systems (particularly cholinergic neurons of the pedunculopontine tegmentum and noradrenergic neurons of the locus coeruleus) provide sustained depolarizing input, holding thalamic relay neurons above -60 mV. At this potential, T-type channels are in a state of **sustained inactivation**—they cannot be activated. Relay neurons respond to sensory input in a standard, linear fashion—faithfully transmitting what they receive, with high signal fidelity.

Burst mode: During sleep, arousal input withdraws, and the membrane potential drops below -70 mV for a sufficiently long period, allowing T-type channels to **de-inactivate** (recover to the activatable state). Any small depolarizing input then triggers a **low-threshold calcium spike (LTS)**—a slow (~10–30 ms), calcium-mediated depolarization topped by a burst of fast sodium action potentials (typically 2–8 spikes at ~200–400 Hz). After the LTS, T-type channels inactivate again, AHP drives the membrane potential back below -70 mV, T-type channels de-inactivate again... and the cycle repeats, producing spontaneous oscillation.

The oscillation frequency is determined by: the T-type channel de-inactivation time constant (50–100 ms), the AHP time constant (set by SK potassium channels, ~50–200 ms), and passive membrane parameters (C_m, g_{leak}). According to experimental measurements by McCormick and Huguenard[16] and computational models by Destexhe and colleagues[17], the spontaneous oscillation frequency of thalamic neurons ranges from 1–4 Hz (δ band) to 7–14 Hz (spindle/σ band).

2.3.2. The Thalamic Reticular Nucleus (TRN) — The Oscillation Pacemaker

The thalamic reticular nucleus (TRN) is a thin shell of GABAergic inhibitory neurons enveloping the lateral aspect of the thalamus. All thalamocortical and corticothalamic axons pass through the TRN, issuing collateral branches that form synapses with TRN neurons as they traverse this structure. The TRN has three critical molecular features:

First, TRN neurons express **exceptionally high densities** of T-type calcium channels—exceeding those in thalamic relay neurons. Their LTS bursts are therefore more powerful, delivering stronger inhibitory volleys.

Second, TRN neurons are interconnected by **electrical synapses (gap junctions)** formed by connexin-36 (Cx36, encoded by the GJD2 gene). Gap junctions have ultrashort transmission delays (<0.5 ms), several times faster than chemical synapses (~1–2 ms). High Cx36 expression in the TRN has been confirmed by multiple studies[18].

Third, the TRN is a purely inhibitory structure—all of its output is GABAergic. It never directly excites its targets; instead, it "sculpts" the firing patterns of thalamic relay neurons through precisely timed inhibition.

These three features together produce the following dynamics: TRN neurons synchronize rapidly via gap junctions → a large population of TRN neurons fires synchronously → a synchronized inhibitory volley is delivered to thalamic relay neurons → relay neurons are hyperpolarized → T-type channels de-inactivate → when inhibition lifts, relay neurons fire LTS bursts → burst signals are transmitted to cortex while simultaneously activating TRN → TRN again inhibits relay neurons... forming a **thalamo-reticular oscillatory loop**. This loop is the generator of sleep spindles (~10–14 Hz) and δ waves (~1–4 Hz)[19].

Cortical excitatory projections to the TRN enable the cortex to **selectively** activate specific TRN sectors, thereby selectively inhibiting irrelevant thalamic channels—this is the molecular basis of the thalamic gating mechanism of **attention**[20][21].

2.3.3. The Intralaminar Nuclei (ILN) and 40 Hz Oscillation

The thalamic **intralaminar nuclei (ILN)**—including the centromedian (CM) and parafascicular (Pf) nuclei—differ fundamentally from other thalamic nuclei. The molecular features of ILN include:

High density of persistent sodium current (I_{NaP}): I_{NaP} is mediated by Nav1.6 (SCN8A) channels and is a subthreshold sodium current that does not rapidly inactivate like the transient sodium current (its inactivation time constant is on the order of seconds). It continuously provides depolarizing drive. The interaction between I_{NaP} and leak currents can produce subthreshold membrane potential oscillations.

P/Q-type calcium channels (CaV2.1, CACNA1A gene): These channels are expressed in the soma and proximal dendrites of ILN neurons and participate in generating intrinsic oscillations.

The activation time constant of I_{NaP} is approximately 3–5 ms, while the recovery time constant of the opposing calcium-dependent potassium current is approximately 15–25 ms. The alternating dominance of these two currents produces intrinsic membrane potential oscillations with a natural frequency of ~30–50 Hz—falling precisely in the **gamma (γ) band**. This mechanism was described in the pioneering work of Llinás and Ribary[22].

The axonal projection pattern of ILN neurons is also distinctive: they project **broadly** to nearly all neocortical areas, and their terminals are concentrated in **Layer 1 and upper Layer 5**—precisely where the apical dendritic tuft and calcium initiation zone of L5tt-PNs are located.

Core inference: The ~40 Hz oscillation of the ILN directly drives the apical dendrites of cortical L5tt-PNs, modulating apical dendritic excitability at 40 Hz. Combined with the θ-rhythmic refractory period of BAC firing, this produces θ-phase-modulated γ bursts—i.e., θ-γ PAC.

2.3.4. Physical Delays and Resonance Frequency of the Thalamocortical Loop

Thalamocortical axons are predominantly myelinated fibers with conduction velocities of approximately 5–30 m/s (depending on fiber diameter and myelin thickness). The physical distance from thalamus to cortex is approximately 2–5 cm (depending on the specific nucleus and cortical area).

Using median values to estimate single-trip conduction time:

$$\tau_{\text{conduction}} = \frac{d}{v} = \frac{0.03\ \text{m}}{15\ \text{m/s}} = 2\ \text{ms}$$

Synaptic delay (including transmitter release and receptor activation): $\tau_{\text{synaptic}} \approx 1\text{–}2\text{ms}$

Postsynaptic integration time (time for EPSP to reach threshold and trigger an action potential): $\tau_{\text{integration}} \approx 3\text{–}8\text{ms}$

Complete thalamus → cortex → thalamus loop time:

$$\tau_{\text{loop}} = 2(\tau_{\text{conduction}} + \tau_{\text{synaptic}} + \tau_{\text{integration}})$$

With intermediate values ($\tau_{\text{conduction}} = 3\ \text{ms}$, $\tau_{\text{synaptic}} = 1.5\text{ms}$, $\tau_{\text{integration}} = 5\text{ms}$):

$$\tau_{\text{loop}} = 2(3 + 1.5 + 5) = 19\ \text{ms}$$

With slower values ($\tau_{\text{conduction}} = 5\ \text{ms}$, $\tau_{\text{synaptic}} = 2\text{ms}$, $\tau_{\text{integration}} = 7\text{ms}$):

$$\tau_{\text{loop}} = 2(5 + 2 + 7) = 28\ \text{ms}$$

The reciprocal of the loop time yields the resonance frequency:

$$f_{\text{resonance}} = \frac{1}{\tau_{\text{loop}}} \approx \frac{1}{19\text{–}28\ \text{ms}} \approx 36\text{–}53\ \text{Hz}$$

This matches the γ band (30–50 Hz) precisely.

2.4. Cortical Recurrent Connections — The Central Role of NMDA Receptors

2.4.1. Molecular Asymmetry of Feedforward and Feedback Connections

Cortical feedforward connections (lower → higher areas, e.g., V1 → V2 → V4 → IT) and feedback connections (higher → lower) exhibit a critical, experimentally quantified asymmetry in **synaptic receptor composition**:

Feedforward synapses have a high AMPA/NMDA current ratio. Multiple independent laboratories have demonstrated that the postsynaptic current at feedforward connections is dominated by the AMPA component. AMPA receptors (GluA1–4, encoded by GRIA1–4 genes) are characterized by ultrafast activation (<1 ms), rapid desensitization (decay time constant ~2–5 ms), and a linear current-voltage relationship. Sherman and colleagues have systematically characterized feedforward ("driver/Class 1") versus feedback ("modulator/Class 2") synapse properties[23][24].

Feedback synapses have a low AMPA/NMDA current ratio. Feedback connections have a relatively stronger NMDA receptor component. Particularly in Layer 1 (the primary termination zone of feedback connections), NMDA receptor density is notably high.

2.4.2. The Unique Biophysics of NMDA Receptors — A Natural "AND Gate"

NMDA receptors (GluN family) possess a property that is exceedingly rare across the entire ion channel superfamily: **voltage-dependent magnesium ion block (Mg^{2+} block)**. This phenomenon was independently discovered by Mayer, Westbrook, and Guthrie[25] and by Nowak and colleagues[26].

At the resting membrane potential (-70 mV), even when glutamate has bound to the NMDA receptor, the channel remains physically blocked by a Mg^{2+} ion that is electrostatically trapped within the channel pore. Only when the membrane potential is depolarized beyond approximately -40 mV is the Mg^{2+} "expelled" from the channel by the electric field, allowing Ca^{2+} and Na^{+} to flow inward. The voltage dependence of the Mg^{2+} block can be described by a Boltzmann equation:

$$g_{\mathrm{NMDA}}(V) = \bar{g}_{\mathrm{NMDA}} \cdot \frac{1}{1 + [\mathrm{Mg}^{2+}]_o / K_d \cdot \exp(-\delta z F V / RT)}$$

where $[\mathrm{Mg}^{2+}]_o$ is the extracellular Mg^{2+} concentration (~1–2 mM), $K_d$is the dissociation constant for Mg^{2+}, $\delta$is the effective fraction of the electric field sensed by Mg^{2+} (~0.8), $z$is the valence of Mg^{2+} (+2), $F$is Faraday's constant, $R$is the gas constant, and $T$is absolute temperature.

The NMDA receptor is therefore a natural "AND gate"—it requires two conditions simultaneously for channel opening: presynaptic glutamate release (indicating that a signal has arrived) and postsynaptic depolarization (indicating that another signal has already made this region active).

This constitutes one of the molecular foundations of BAC firing coincidence detection: the voltage dependence of NMDA receptors at apical synapses enforces the logical requirement that "feedforward signal must arrive first."

2.4.3. Regional Distribution Differences of GluN2 Subunits

NMDA receptors are assembled from two GluN1 subunits and two GluN2 subunits. GluN2 has four subtypes (A/B/C/D), each conferring distinct kinetic properties:

GluN2A (GRIN2A gene): Decay time constant ~30–50 ms, strong Mg^{2+} block, high open probability. Predominant at Layer 4 synapses (feedforward pathway) in the adult cortex.

GluN2B (GRIN2B gene): Decay time constant ~200–300 ms (4–6 times longer than GluN2A), relatively weaker Mg^{2+} block, higher Ca^{2+} permeability. More abundant in feedback synapses and in higher-order association cortices, particularly prefrontal cortex[27].

The enrichment of GluN2B in prefrontal cortex has profound functional implications: its ultralong decay time (~300 ms ≈ one complete θ cycle) is believed to be one of the molecular foundations for sustained information maintenance in working memory—GluN2B-mediated currents can "hold" neuronal activity throughout a θ cycle until the next cycle's fresh input arrives[27]. As will be discussed in Chapter 6, this ~200–300 ms temporal buffering capacity provided by NMDA receptors constitutes the minimal form of "memory" that is likely a necessary condition for consciousness.

2.5. The Claustrum — Molecular Basis of Global Synchronization

2.5.1. Anatomy and Molecular Features

The claustrum is a thin sheet-like structure located deep to the insular cortex and lateral to the putamen. Francis Crick and Christof Koch proposed in an influential paper that the claustrum may serve as the "conductor of consciousness"[28].

The molecular uniqueness of the claustrum includes:

Extremely high expression of Gnb4: The Gnb4 gene encodes the G-protein β4 subunit and is expressed in the claustrum at levels far exceeding any other brain region. This finding has been confirmed in mice by multiple independent studies[29]. The G-protein β4 subunit participates in regulating GIRK channels (G-protein-activated inwardly rectifying potassium channels, KCNJ gene family), whose opening hyperpolarizes neurons. High Gnb4 expression may render claustrum neurons particularly sensitive to neuromodulatory signals mediated by G-protein pathways.

High density of Parvalbumin-positive (PV+) inhibitory interneurons: PV+ interneurons are fast-spiking GABAergic cells that synchronize surrounding excitatory neurons through precise perisomatic inhibition. The abundance of PV+ interneurons in the claustrum enables it to produce robust and precisely timed gamma-rhythmic output.

Cx36-mediated electrical synapses: Gap junction connections between claustrum neurons enable ultrafast electrical coupling and internal synchronization.

Extraordinarily broad projections: The claustrum sends projections to nearly all neocortical areas and receives input from nearly all neocortical areas.

2.5.2. Functional Model of Claustral Global Synchronization

Based on the above molecular features, the following functional model can be constructed: multimodal integration (the claustrum naturally detects "cross-regional coherence"), synchronous re-transmission (claustrum neurons synchronize rapidly through internal gap junctions and transmit a gamma-rhythmic phase-reset pulse back to all cortical areas), and global phase alignment (during each θ cycle, whenever multiple cortical areas are synchronously active, the claustrum sends a global gamma phase-reset pulse achieving brain-wide phase alignment).

2.5.3. Is the Claustrum Absolutely Necessary?

From the biophysical analysis, the function provided by the claustrum (global phase synchronization) could in principle be partially realized by other mechanisms: the broad projections of the thalamic ILN, long-range cortico-cortical connections, and ephaptic coupling. This suggests the claustrum may be an **efficiency enhancer** rather than an absolute requirement, consistent with limited human clinical evidence (Chau et al., 2015).

2.6. Electromagnetic Field Effects (Ephaptic Coupling) — An Underappreciated Synchronization Mechanism

2.6.1. Physical Principles

When a neuron fires an action potential, the transmembrane ionic currents generate a local electric field in the extracellular fluid. Although weak (~0.1–1 mV/mm), this field can influence the membrane potential of nearby neurons—synchronously depolarizing or hyperpolarizing neurons that are aligned in parallel. This synapse-independent mechanism is called **ephaptic coupling**.

$$\nabla^2 \phi_e = -\frac{I_m}{\sigma_e}$$

where ϕ_e is the extracellular potential, I_m is the volume current source density, and σ_e is the extracellular conductivity (~0.3 S/m).

2.6.2. Relevance in the Cortex

L5 pyramidal neurons have their apical dendrites **aligned in parallel**, maximizing ephaptic coupling efficiency. Anastassiou and colleagues[30] showed that endogenous cortical LFP fields can shift a neuron's firing time by 1–5 ms—enough to influence PAC phase precision. Within the MSTRT framework, ephaptic coupling should be considered as an **auxiliary synchronization mechanism**.

2.7. Rigorous Assessment of Quantum Effects

2.7.1. The Penrose-Hameroff Microtubule Quantum Theory

Penrose and Hameroff proposed the Orchestrated Objective Reduction (Orch OR) theory, positing quantum superposition states in tubulin proteins within microtubules as the physical basis of consciousness[31][32].

2.7.2. The Decoherence Problem

Max Tegmark[33] calculated that quantum superposition states in the brain decohere in approximately 10^{-13}seconds—roughly ten orders of magnitude faster than any neural process. Two developments deserve mention: room-temperature quantum coherence reported in photosynthesis[34] (though

subsequent studies have disputed the interpretation) and Matthew Fisher's[35] nuclear spin hypothesis for phosphorus-31 in Posner molecules.

2.7.3. Implications for MSTRT

All processes described by MSTRT lie entirely within the domain of classical physics. The smallest energy scales involved (~$k_B T \approx 4 \times 10^{-21}$ J at 37°C) are far larger than any perturbation quantum uncertainty could introduce. **MSTRT does not require quantum mechanics as a foundation.**

2.8. Thermodynamic Perspective — Consciousness as a Dissipative Structure

2.8.1. Order Far from Equilibrium

Neural oscillations can be viewed as dissipative structures in the sense of Prigogine—ordered spatiotemporal patterns maintained by continuous energy input. The brain consumes approximately 20 watts; once the energy supply is interrupted, oscillations collapse within seconds.

2.8.2. Energy Cost Estimate for BAC Firing

A single BAC firing event requires approximately 2×10^7 ATP molecules, corresponding to approximately 1.7×10^{-12} J. If roughly 5×10^7 L5tt-PNs are in the BAC firing state at ~4 events per second, the total power is approximately 0.34 mW—roughly 0.002% of total brain energy consumption. The consciousness-specific BAC firing process is energetically "cheap."

2.9. Neuromodulation as Gain Control on BAC Firing

All major neuromodulatory systems converge on modulating the probability of BAC firing and can be formalized as a single multiplicative gain parameter g_{mod}.

Cholinergic system (basal forebrain → cortex): Muscarinic receptors (M1-type) enhance apical dendritic excitability by suppressing M-type potassium currents, lowering the calcium spike threshold. Nicotinic receptors on VIP+ interneurons activate VIP→SST disinhibition. Both effects increase g_{mod}.

Noradrenergic system (locus coeruleus → cortex): Moderate concentrations enhance signal-to-noise ratio via α2A-adrenergic receptors. High concentrations (stress) nonspecifically increase excitability, reducing selectivity. This corresponds to the Yerkes-Dodson inverted-U.

Serotonergic system (raphe nuclei → cortex): 5-HT2A activation lowers BAC threshold (increasing g_{mod} but reducing selectivity); 5-HT1A activation hyperpolarizes the soma (decreasing g_{mod}).

Dopaminergic system (VTA/SNc → prefrontal cortex): D1 receptor activation enhances NMDA receptor currents and persistent firing, affecting the temporal precision and persistence of BAC firing.

The general framework:

$$g_{\text{mod}} = g_{\text{ACh}} \cdot g_{\text{NE}} \cdot g_{\text{5-HT}} \cdot g_{\text{DA}}$$

In deep sleep, all arousal-related neuromodulatory systems withdraw ($g_{\text{mod}} \to g_{\text{min}}$), BAC firing probability drops, PAC collapses, and consciousness is lost. As will be discussed in Chapter 6, these neuromodulatory systems are not motivationally neutral—each is intimately linked to survival-relevant drives—creating a deep entanglement between the gain mechanism that enables consciousness and the motivational architecture that directs behavior.

Chapter 3: Mathematical Framework

3.1. Overview

The mathematical framework of MSTRT comprises three tiers: the **structural tier** (network topology, time constant distributions, connection types), the **dynamic tier** (PAC strength, nonlinear coupling, causal directionality), and the **composite tier** (integrating structure and dynamics into a quantifiable consciousness index).

doi.org/10.32388/YKIRJL

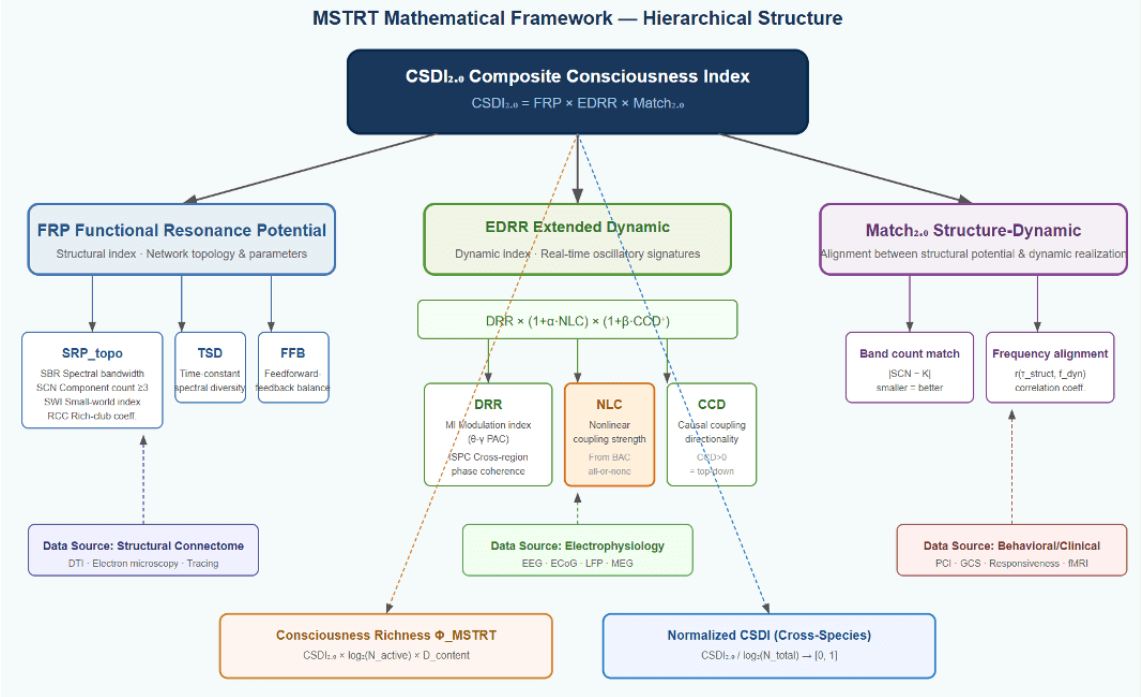

Figure 3. Hierarchical structure of the MSTRT mathematical framework. The composite consciousness index $CSDI_{2.0}$ (top, dark blue box) is the product of three components: the **structural index FRP (Functional Resonance Potential)** (left, blue branch), composed of the topological sub-index SRP_{topo} (containing spectral bandwidth ratio SBR, spectral component number $SCN \geq 3$, small-world index SWI, and rich-club coefficient RCC), time-constant spectral diversity TSD, and feedforward-feedback balance FFB; the **dynamic index EDRR (Extended Dynamic Resonance Realization)** (center, green branch), which multiplies the baseline dynamic resonance realization DRR (containing modulation index MI and cross-region inter-site phase clustering ISPC) by gain terms from nonlinear coupling strength NLC (orange highlight, arising from BAC firing's all-or-none threshold) and causal coupling directionality CCD (CCD > 0 indicates top-down dominance); and the **structure-dynamic alignment index $Match_{2.0}$** (right, purple branch), which quantifies the match between structurally expected and dynamically observed frequency band counts and the correlation between structural time constants and dynamic oscillation frequencies. The bottom shows three data source types (structural connectome, electrophysiology, behavioral/clinical data) feeding into their corresponding indices. Two derived metrics — consciousness richness Φ_{MSTRT} and normalized CSDI — extend from the top index via dashed lines, used respectively for quantifying the information capacity of experience and for cross-species comparison.

doi.org/10.32388/YKIRJL

3.2. Structural Index: Functional Resonance Potential (FRP)

3.2.1. Topological Sub-index (SRP_topo)

(i) Spectral Bandwidth Ratio (SBR): From the graph Laplacian $L = D - A$and its eigenvalue spectrum $\{\lambda_1 = 0, \lambda_2, \ldots, \lambda_N\}$:

$$\mathrm{SBR} = \frac{\lambda_N - \lambda_2}{\lambda_{N,\max} - \lambda_{2,\min}}$$

(ii) Spectral Component Number (SCN): The number of distinct eigenvalue clusters, corresponding to the number of independent temporal scales the network topology can support. MSTRT predicts SCN ≥ 3 for consciousness.

(iii) Small-World Index (SWI):

$$\mathrm{SWI} = \frac{C/C_{\mathrm{random}}}{L/L_{\mathrm{random}}}$$

The human brain white-matter connectome has SWI ≈ 3–5[36].

(iv) Rich-Club Coefficient (RCC):

$$\mathrm{RCC}(k) = \frac{\phi(k)}{\phi_{\mathrm{random}}(k)}$$

Composite:

$$\mathrm{SRP}_{\mathrm{topo}} = \mathrm{SBR}^{w_1} \times \mathrm{SWI}^{w_2} \times \mathrm{RCC}^{w_3} \times f(\mathrm{SCN})$$

3.2.2. Time Constant Spectral Diversity (TSD)

$$\mathrm{TSD} = \frac{-\sum_{k=1}^{N_{\mathrm{bins}}} p_k \log_2 p_k}{\log_2 N_{\mathrm{bins}}}$$

TSD ranges from 0 (all time constants identical) to 1 (uniformly distributed).

3.2.3. Feedforward-Feedback Balance Index (FFB)

$$\mathrm{FFB} = 1 - \left| \frac{N_{\mathrm{FF}} - N_{\mathrm{FB}}}{N_{\mathrm{FF}} + N_{\mathrm{FB}}} \right|$$

3.2.4. Complete Definition of FRP

$$\mathrm{FRP} = \mathrm{SRP}_{\mathrm{topo}} \times \mathrm{TSD} \times \mathrm{FFB}$$

3.3. Dynamic Index: Extended Dynamic Resonance Realization (EDRR)

3.3.1. Baseline PAC Measurement

Using the Modulation Index (MI) of Tort et al.[37]:

$$\mathrm{MI}_{ij}(f_s, f_f) = \frac{D_{KL}(P \parallel U)}{\log_2 N_{\text{bins}}}$$

3.3.2. Cross-Regional Phase Consistency (ISPC)

$$\mathrm{ISPC}_{ij}(f) = \left| \frac{1}{T} \sum_{t=1}^{T} e^{i[\phi_f^i(t) - \phi_f^j(t)]} \right|$$

3.3.3. Baseline DRR

$$\mathrm{DRR} = K \times \left(\frac{1}{K} \sum_{l=1}^{K} \bar{\mathrm{MI}}_l \right) \times \left(\frac{1}{\binom{K}{2}} \sum_{l<l'} \bar{\mathrm{ISPC}}_{ll'} \right)$$

3.3.4. Nonlinear Coupling Strength (NLC)

NLC = residual mutual information = $I(A_f; \phi_s) - I_{\text{linear}}$. NLC > 0 implies a nonlinear mechanism such as BAC firing.

3.3.5. Causal Coupling Directionality (CCD)

Using Transfer Entropy (TE):

$$\mathrm{CCD} = \frac{TE(\phi_s \to A_f) - TE(A_f \to \phi_s)}{TE(\phi_s \to A_f) + TE(A_f \to \phi_s)}$$

CCD > 0 indicates top-down dominance—the hallmark of the conscious state.

3.3.6. Complete Definition of EDRR

$$\mathrm{EDRR} = \mathrm{DRR} \times (1 + \alpha \cdot \mathrm{NLC}) \times (1 + \beta \cdot \mathrm{CCD}^{+})$$

3.4. Composite Consciousness Index: CSDI₂.₀

$$\mathrm{CSDI}_{2.0} = \mathrm{FRP} \times \mathrm{EDRR} \times \mathrm{Match}_{2.0}$$

where:

$$\text{Match}_{2.0} = \left(1 - \frac{|\text{SCN} - K|}{\max(\text{SCN}, K)}\right) \times r(\tau_{\text{struct}}, f_{\text{dyn}})$$

3.5. Formalization of Sufficient and Necessary Conditions for Consciousness

3.5.1. Necessary Conditions

N1 (Functional structural capacity): FRP > θ_{FRP}.

N2 (Nonlinear dynamic resonance): EDRR > θ_{EDRR}, with NLC > 0 and CCD > 0.

N3 (Energy supply): Sustained energy input to maintain far-from-equilibrium state.

N4 (Information capacity): $N \geq N_{\min}$ (preliminary: 10^3–10^5).

3.5.2. Sufficient Condition

S1: When N1–N4 are simultaneously satisfied and $\text{CSDI}_{2.0} > \theta_{\text{CSDI}}$, the system possesses some form of conscious experience.

3.5.3. Consciousness Richness Formula

$$\Phi_{\text{MSTRT}} = \text{CSDI}_{2.0} \times \log_2(N_{\text{active}}) \times D_{\text{content}}$$

where:

$$D_{\text{content}} = \frac{1}{n_\theta} \sum_{t=1}^{n_\theta} H(\mathbf{x}_t \mid \phi_\theta(t))$$

3.5.4. Normalized CSDI for Cross-Species Comparison

$$\text{CSDI}_{2.0}^{\text{norm}} = \frac{\text{CSDI}_{2.0}}{\log_2(N_{\text{total}})}$$

This yields a value between 0 and 1 representing "consciousness efficiency," potentially revealing, for example, that corvids achieve comparable normalized CSDI to mammals despite smaller absolute brain size[38].

Chapter 4: Rigorous Analysis of Structural Necessity

4.1. Analytical Method — Three Dimensions of Substitutability

For each consciousness-related structure/mechanism, three questions are systematically addressed:

Dimension A (Functional necessity): Is this structure's function a logical prerequisite for consciousness?

Dimension B (Implementation uniqueness): Is this specific physical/chemical implementation the only possible route?

Dimension C (Parameter sensitivity): How wide is the permissible range of critical parameters?

4.2. Substitutability of BAC Firing

Dimension A: The core function—coincidence detection of two signals from different sources and temporal scales with all-or-none output—is almost certainly necessary.

Dimension B: The specific molecular implementation is not unique, but the functional pattern of all-or-none nonlinear coincidence detection + refractory period → θ-γ nesting is necessary.

Dimension C — Temporal Grain of Consciousness: The refractory period (~200–300 ms) sets the θ frequency and may determine the "temporal grain" of consciousness. In humans, the ~4–6 Hz theta corresponds to ~170–250 ms, matching the psychophysical temporal integration window for conscious visual binding[39]. Cross-species differences are predicted: rodent hippocampal theta at ~6–10 Hz implies a faster "frame rate" but lower resolution per frame. If human theta at ~5 Hz accommodates ~8 gamma cycles at 40 Hz, while mouse theta at ~8 Hz accommodates ~5 gamma cycles, humans encode ~8 content "slots" per conscious frame versus ~5 for mice, potentially relating to working memory capacity differences.

Furthermore, EEG microstates—quasi-stable scalp topographies lasting ~60–120 ms[40]—have a duration corresponding to approximately half a theta cycle, suggesting each theta cycle accommodates 2–3 successive microstates. Microstate duration should correlate with theta frequency (faster theta → shorter microstates).

4.3. Substitutability of Thalamocortical Circuits

The function of brain-wide synchronization is likely necessary, but could in principle be partially achieved through sufficiently strong intracortical coupling. The thalamus is an efficiency enhancer but may not be the only possible route. Thalamocortical loop delay (~20–30 ms) sets γ-band resonance, but nesting between slow and fast frequencies could persist at different frequencies.

4.4. Substitutability of NMDA Receptor Function

NMDA receptors widen the coincidence window and provide AND-gate functionality. They may not be absolutely necessary, but their removal would drastically narrow the coincidence window (from ~30 ms to ~5 ms) and significantly destabilize consciousness.

4.5. Substitutability of the Six-Layer Cortical Architecture

Functional differentiation of signal pathways is necessary (at least two functionally distinct pathways + a convergence point), but the six-layer architecture is a specific evolutionary solution. The avian pallium demonstrates that non-layered structures can support higher cognition[38].

4.6. Summary of Substitutability

Most rigid: Nonlinear coincidence detection; coexistence of multiple temporal scales (≥3); recurrent/feedback processing; global integration. **Moderately rigid:** Coincidence window width (~5–30 ms); refractory period (~100–500 ms); NMDA-like slow synapses. **Flexible:** Specific ion channel types; specific spatial architectures; specific global synchronization mechanisms; physical substrate.

Chapter 5: Minimal Functional Specifications and Simplified Structures

5.1. Minimal Functional Specifications (MFS)

Six substrate-independent functional requirements for consciousness:

MFS-1: Multi-Temporal-Scale Processing. The system must simultaneously process information at no fewer than three distinct temporal scales with adjacent-scale ratios of at least ~3–5 fold. This specification implicitly contains a minimal temporal buffering requirement: each processing unit at the slowest scale must maintain information persistence for at least one full cycle of its characteristic frequency, providing the temporal "thickness" without which experience has no duration (see Chapter 6, Section 6.3.5 for detailed analysis).

MFS-2: Nonlinear Coincidence Coupling. Signals from different temporal scales must undergo coincidence detection at some locus, producing a supralinear (preferably all-or-none) coupling signal. Biological implementation: BAC firing in L5tt-PNs.

MFS-3: Recurrent Processing. Signals must circulate within the system—higher-level outputs must feed back into lower-level inputs, forming persistent loops. Biological implementation: Cortico-cortical feedback connections; thalamocortical loops.

MFS-4: Global Integration. Multiple local coincidence detection units must achieve global synchronization through some mechanism. Biological implementation: Broad projections of the thalamic ILN + claustral phase resetting + ephaptic coupling.

MFS-5: Sustained Energy/Activation Supply. The system requires a continuous driving force to maintain an active state far from equilibrium. Biological implementation: Brainstem reticular activating system + aerobic metabolism. In all known biological implementations, the activation supply systems are intrinsically linked to motivational drive circuits (see Chapter 6, Section 6.4.7 for analysis of this entanglement and its implications).

MFS-6: Sufficient Information Capacity. The system must contain enough processing units: at least ~30–100 synchronized oscillators per frequency band, ~100 distinguishable conscious content patterns requiring $N \approx 3,000 - 10,000$fast units, total $N_{\min} \approx 5,000 - 15,000$.

5.2. Theoretical Design of a Minimal Conscious System

5.2.1. Three-Layer Architecture

Layer A (fast layer): $N_A \approx 5,000$–$10,000$fast processing units, $\tau_A \sim 5$ms. Functional equivalent: cortical feedforward pathway.

Layer B (slow layer): $N_B \approx 1,000$–$3,000$slow processing units, $\tau_B \sim 200$ms. Functional equivalent: cortical feedback pathway.

Layer C (ultra-slow integration layer): $N_C \approx 10$–100high-degree hub units, $\tau_C \sim 1,000$ms. Functional equivalent: thalamus/claustrum.

Each unit in Layer A has two integration zones—one receiving local Layer A input, the other receiving Layer B feedback input. When both arrive within $\Delta t < 30$ms, a nonlinear burst output is produced.

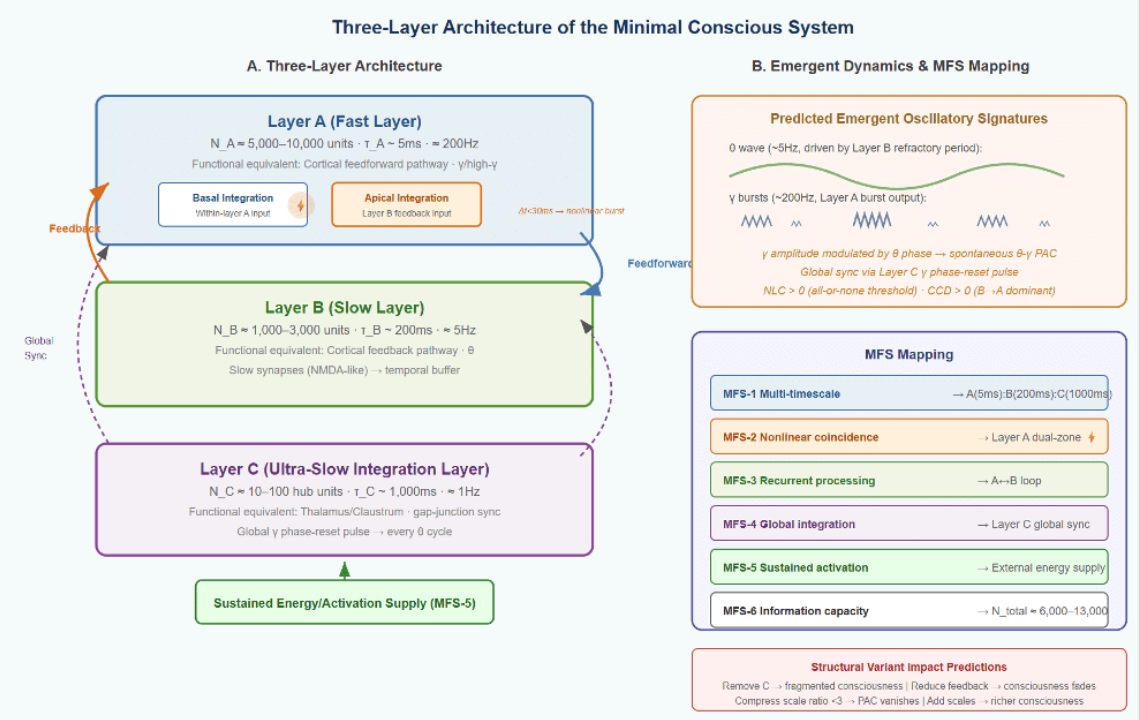

Figure 4. Three-layer architecture of the minimal conscious system.(A) Schematic of the three-layer design. **Layer A** (blue, fast layer) contains approximately 5,000–10,000 fast processing units (τ ~ 5ms, corresponding to γ/high-γ bands), functionally equivalent to the cortical feedforward pathway. Each Layer A unit contains two integration zones — the basal integration zone receives within-layer A input, while the apical integration zone receives Layer B feedback input; when both zones reach threshold within $\Delta t < 30$ms, they produce a nonlinear burst output (marked by the lightning symbol). **Layer B** (green, slow layer) contains approximately 1,000–3,000 slow processing units (τ ~ 200ms, corresponding to the θ band), functionally equivalent to cortical feedback pathways, using NMDA-like slow synapses to provide a temporal buffer. **Layer C** (purple, ultra-slow integration layer) contains approximately 10–100 highly connected hub units (τ ~ 1,000ms), functionally equivalent to the thalamus/claustrum, synchronized internally via gap junctions and sending global γ phase-reset pulses to Layers A and B. Orange and blue arrows denote feedback (B→A) and feedforward (A→B) connections respectively; purple dashed arrows represent Layer C's global synchronizing projections. The bottom green box represents the sustained energy/activation supply required by MFS-5. **(B)** Predicted emergent oscillatory signatures and MFS mapping. The upper box shows predicted spontaneous θ-γ nesting: the θ wave is driven by Layer B's refractory dynamics (green slow wave), γ bursts are produced by Layer A's nonlinear output (blue fast wave), γ amplitude is modulated by θ phase, NLC > 0 (from all-or-none threshold), and CCD > 0 (B→A feedback dominance). The lower box maps each of the six MFS requirements to specific components of the three-layer architecture. The bottom red box lists the predicted impacts of four structural variants, suitable for validation via computational simulation (Experimental Prediction 3).

doi.org/10.32388/YKIRJL

5.2.2. Impact Analysis of Structural Variants

Removing Layer C: local PAC persists but global synchronization is lost → possible "consciousness fragments." Reducing feedback connections: BAC firing rate decreases, PAC weakens continuously → consciousness gradually fades. Compressing the time scale ratio below ~3: frequency locking → PAC disappears → consciousness lost. Adding more temporal scales: richer nesting → richer consciousness.

Chapter 6: Sensory Input, Memory, and Motivational Drive — Necessary Conditions or Content Sources?

6.1. Overview and Motivation

The preceding chapters establish the mechanistic architecture of MSTRT—the biophysical processes, mathematical indices, structural requirements, and minimal functional specifications that together constitute the theory's account of how consciousness is generated. This chapter addresses a complementary but equally fundamental question: **what content sources does consciousness require?** Specifically, it examines whether three commonly assumed requirements—sensory input, memory, and motivational drive—are truly necessary conditions for consciousness, or whether they are contingent content sources that shape what consciousness is about without being essential to its existence.

This distinction matters profoundly for the MSTRT framework because it determines the scope of the theory's predictions. If external sensory input were necessary, MSTRT would predict that any system lacking sensory transducers cannot be conscious. If long-term memory were necessary, MSTRT would predict that severely amnestic patients lack consciousness. If motivational drive were necessary, MSTRT would predict that artificial systems without homeostatic needs cannot be conscious. Each of these predictions carries substantial clinical, ethical, and engineering consequences, and each turns out to require careful empirical evaluation rather than assumption.

The three domains together span the temporal orientations of consciousness: sensory input grounds consciousness in the present, memory connects it to the past, and motivational drive orients it toward the future. The analysis below subjects each domain to a structured evaluation drawing on clinical neurology, experimental psychology, contemplative neuroscience, and comparative neurobiology, then maps the results back onto the MSTRT architecture.

6.2. Sensory Input

6.2.1. The Question

If all external sensory input were removed—no vision, hearing, touch, smell, taste, proprioception, vestibular input—would consciousness cease?

6.2.2. Evidence from Sensory Deprivation

The earliest systematic studies were conducted at McGill University in the 1950s by Donald Hebb, Woodburn Heron, and W.H. Bexton. Participants placed in environments of radically reduced sensory input (translucent goggles, white noise, padded surfaces) did not lose consciousness. Instead, after several hours, subjects began experiencing vivid hallucinations—visual patterns, formed images, and complex scenes. Similar findings emerged from John Lilly's isolation tank experiments, where subjects floated in body-temperature salt water in complete darkness and silence. Consciousness persisted robustly, and participants reported rich phenomenal experience generated entirely from within.

These results demonstrate that when external input is removed, the brain does not go dark—it begins manufacturing its own content. This strongly suggests that external sensory input is a source of conscious content, not a prerequisite for consciousness itself.

6.2.3. Evidence from Dreaming

Perhaps the most compelling evidence comes from ordinary dreaming. During REM sleep, the thalamus actively gates out external sensory input, a phenomenon documented by Rodolfo Llinás and Denis Paré[41]. Despite this near-total sensory blockade, dreamers experience vivid, immersive conscious states. J. Allan Hobson's Activation-Input-Modulation (AIM) model explicitly captures this: the "Input" dimension varies independently of the "Activation" dimension that tracks consciousness level.

Crucially for MSTRT, the neural oscillatory mechanisms operating during dreaming closely resemble those during waking consciousness. Theta-gamma phase-amplitude coupling is prominent during REM sleep. The hippocampus generates theta rhythms, cortical gamma activity nests within them, and the result is coherent conscious experience—all without meaningful external sensory input.

6.2.4. Evidence from Deafferentation and Neurological Cases

Ian Waterman, documented by Jonathan Cole[42], lost all proprioception and light touch sensation from the neck down, yet his consciousness was completely intact. Locked-in syndrome patients with ventral pontine lesions are almost entirely cut off from motor output and have severely reduced sensory processing, yet careful examination reveals they are fully conscious. Jean-Dominique Bauby's memoir *The Diving Bell and the Butterfly* (1997) provides vivid first-person testimony of consciousness persisting despite radical sensory-motor disconnection.

6.2.5. Blindsight: The Reverse Dissociation

Blindsight, first systematically studied by Lawrence Weiskrantz[43], provides the complementary dissociation. Patients with V1 damage can respond to visual stimuli in their blind field while denying any conscious visual experience. Sensory information enters the brain and influences behavior, yet consciousness of that information is absent. This demonstrates that sensory input is not sufficient for conscious experience either—the information must be processed by the BAC firing / theta-gamma PAC mechanism to become conscious.

6.2.6. Mapping to MSTRT

Within MSTRT, the feedforward input that drives the bottom-up component of BAC firing (the basal dendritic depolarization) can originate from multiple sources: sensory thalamic relay nuclei, hippocampal replay signals, cortical association areas generating predictions, or brainstem neuromodulatory drive. The BAC firing mechanism is agnostic to the source of its inputs. What matters is that sufficient basal depolarization coincides with sufficient apical depolarization within the theta-defined temporal window. External sensory input is one way—but only one way—to achieve this coincidence.

6.2.7. Verdict

External sensory input is **not a necessary condition** for consciousness. It is one of several possible sources of information that can populate conscious experience, but internally generated activity can substitute for it entirely. This is one of the clearest empirical findings among the three domains examined.

6.3. Memory

6.3.1. The Question

Memory is not a single system. The neuroscience of memory distinguishes at least five major types: episodic memory (events), semantic memory (facts and knowledge), procedural memory (skills), working memory (active maintenance over seconds), and ultra-short-term sensory memory (milliseconds to seconds). The question of whether "memory" is necessary for consciousness yields radically different answers depending on which type is meant.

6.3.2. Long-Term Episodic Memory Is Not Necessary

The single most decisive piece of evidence comes from patient H.M. (Henry Molaison), studied by Brenda Milner beginning in 1957 and by Suzanne Corkin for decades afterward[44]. After bilateral medial temporal lobe resection, H.M. lost the ability to form any new conscious long-term memories. He lived in a perpetual present. Yet every examiner who worked with him confirmed he was fully, vividly conscious in the moment—he could hold conversations, make jokes, reason about problems, experience emotions.

Clive Wearing, a British musician who suffered herpes simplex encephalitis destroying most of his hippocampus, presents an even more extreme case. His diary is filled with entries reading "NOW I am truly conscious for the first time"—because every few seconds he forgets having been conscious before. Yet he is conscious at every moment.

Pharmacological evidence reinforces this: midazolam produces dense anterograde amnesia while preserving consciousness. Patients remain awake, responsive, and capable of following commands during procedures but recall nothing afterward. Consciousness and long-term memory encoding can be cleanly dissociated.

6.3.3. Semantic Memory Enriches but Is Not Required

A newborn infant possesses essentially zero semantic knowledge yet is clearly conscious—it responds to pain, shows preference for its mother's voice[45], and orients to faces. Cases of semantic dementia confirm that progressive loss of conceptual knowledge impoverishes content, not the capacity for experience.

6.3.4. Working Memory: The Critical Boundary

Working memory appears deeply intertwined with consciousness. Baars and Franklin[46] argued that the contents of working memory essentially are the contents of consciousness. Lavie's load theory[47] shows that manipulations disrupting working memory reduce conscious access to stimuli. The prefrontal-parietal network supporting working memory overlaps extensively with the network activated during conscious perception[48].

However, the strongest claim is not about working memory in the psychological sense but about something more fundamental: the minimal temporal integration that gives experience its "thickness."

6.3.5. Ultra-Short-Term Temporal Buffering: Likely Necessary

William James's concept of the "specious present"[49]—the brief interval over which experience has duration rather than being an infinitely thin point—may represent the minimum temporal structure required for consciousness. Husserl formalized this as the structure of "retention–primal impression–protention."

At the biophysical level, the NMDA receptor provides the molecular mechanism for this minimal temporal buffering. Xiao-Jing Wang's influential 1999[50] computational model showed that the slow decay kinetics of NMDA receptor currents (~100–300 ms, longer for GluN2B-containing receptors) enable persistent activity in recurrent cortical circuits. Without NMDA receptors, neural activity decays too quickly for temporal integration. The ~200–250 ms theta cycle within the MSTRT framework provides the fundamental temporal unit within which gamma-frequency information packets are nested—and it is NMDA dynamics that sustain the neural activity across this duration.

Ernst Pöppel's work on temporal windows of consciousness [51](2009) identified a ~2–3 second integration window as the basic unit of conscious "now," with a finer-grained ~30 ms window for simultaneity perception. Benjamin Libet's classic experiments suggested that conscious awareness requires approximately 500 ms of sustained neural activity—roughly two theta cycles. Though Libet's specific interpretation has been debated, the basic finding that consciousness requires some minimum duration of sustained processing has been repeatedly confirmed by masking studies and attentional blink research[52][53].

6.3.6. Mapping to MSTRT

Within the MSTRT architecture, ultra-short-term temporal buffering is not a separate "memory system" added alongside the core mechanism—it IS part of the core mechanism. MFS-1 (Multi-Temporal-Scale Processing) implicitly requires that the slowest scale maintain information persistence for at least one full cycle, and MFS-2 (Nonlinear Coincidence Coupling) requires that signals from different scales coexist within overlapping temporal windows. The NMDA receptor dynamics that sustain apical dendritic depolarization over the ~200–250 ms theta cycle provide the molecular substrate. Without NMDA receptor function, theta-gamma PAC is disrupted and consciousness is altered or abolished. The "memory" that is necessary for consciousness is thus a biophysical property of the very synapses that implement the coincidence detection mechanism, not a separate cognitive system.

6.3.7. Verdict

Long-term episodic memory is clearly not necessary. Semantic memory and knowledge enrich consciousness but are not required. Working memory in the psychological sense is deeply correlated with consciousness but may not be strictly necessary in all cases. However, **ultra-short-term temporal buffering**—the capacity to integrate information over at least one theta cycle (~200–250 ms)—is very likely a necessary condition, embedded in MFS-1 and MFS-2 through theta-cycle temporal scaffolding and NMDA receptor dynamics.

6.4. Drives, Desires, and Motivation

6.4.1. The Question

This is the most philosophically contentious and empirically uncertain of the three domains. Is some form of motivational drive—desire, wanting, goal-directedness, homeostatic need, or at minimum, valence—a necessary condition for consciousness?

6.4.2. The Panksepp–Solms Position: Affect Is Primordial

Jaak Panksepp[54] argued that the deepest layer of consciousness is affective—raw emotional/motivational states generated by subcortical systems, particularly the brainstem periaqueductal gray (PAG), hypothalamus, and mesolimbic circuits. He identified seven primary affective

systems: SEEKING, RAGE, FEAR, LUST, CARE, PANIC/GRIEF, and PLAY. The SEEKING system (mesolimbic dopamine) was considered most fundamental—the basic exploratory drive.

Mark Solms[55] linked Panksepp's affective neuroscience to Friston's Free Energy Principle, arguing that consciousness IS the felt experience of free energy minimization—the organism's felt need to reduce uncertainty and maintain homeostasis. In this framework, consciousness without desire is literally incoherent.

6.4.3. Evidence from Hydranencephalic Children

Bjorn Merker's[56] paper on children born with hydranencephaly—where the cerebral cortex is almost entirely absent while the brainstem and diencephalon remain intact—presents striking evidence. These children smile in response to familiar voices, show distress when uncomfortable, orient to sounds, display preferences, and express what appears to be pleasure during play. Their behavior is not merely reflexive but shows context-sensitivity and emotional expressiveness. If conscious, their consciousness is entirely subcortical, entirely affective/motivational—suggesting drive-based consciousness may be the most basic form.

6.4.4. Damasio's Somatic Marker Framework

Antonio Damasio[57][58][59] developed a framework in which feelings—body-state representations with inherent motivational valence—are central to consciousness. His proto-self is built from interoceptive representations that are inherently motivational: hunger IS desire for food, pain IS a drive to escape.

6.4.5. The Interoceptive Inference Framework

Anil Seth and Manos Tsakiris[60] proposed that consciousness is fundamentally grounded in interoceptive inference—the brain's ongoing prediction of internal bodily signals—which is inherently homeostatic and motivational. Bud Craig's[61] work on the anterior insular cortex converges on a similar picture: the insula integrates interoceptive signals into a "global emotional moment" that is always valenced and thus always motivational.

6.4.6. The Counter-Argument: Meditative States and Akinetic Mutism

Advanced contemplative practice provides frequently cited counter-examples. Zoran Josipovic's neuroimaging studies[62] (2019) document "non-dual awareness" states characterized by a form of

consciousness that practitioners describe as "pure awareness" without desire or aversion. However, these states are transient; basic physiological drives continue throughout; and the pursuit of such states involves a meta-desire.

Akinetic mutism—bilateral anterior cingulate or medial frontal damage—presents patients who are awake, may track objects, and respond to pain, but initiate no behavior and express no desire. Whether genuine consciousness persists is contested: Damasio argues consciousness itself is diminished, not just motivation.

6.4.7. The Evolutionary Entanglement Argument

The brainstem arousal systems that MSTRT identifies under MFS-5 are not motivationally neutral. The reticular activating system[63] is anatomically and neurochemically intertwined with drive circuits. The locus coeruleus (norepinephrine) regulates vigilance and threat detection. The ventral tegmental area (dopamine) is the core of the reward/seeking system. The raphe nuclei (serotonin) regulate mood and satiety. The parabrachial nucleus processes pain, taste, and visceral signals—all motivationally charged.

There is no known biological arousal system that is motivationally neutral. The neuromodulatory parameters captured in MSTRT's g_{mod}gain term (Section 2.9) are simultaneously regulators of consciousness level AND regulators of motivational state. This creates a deep architectural entanglement: the gain parameter that enables consciousness is the same parameter that implements motivational drive. You cannot activate g_{mod}without simultaneously activating some degree of motivational bias.

6.4.8. Mapping to MSTRT

MFS-5 (Sustained Energy/Activation Supply) is the specification most directly relevant. The g_{mod}gain term controls whether BAC firing—and consciousness—can occur. But $g_{\text{mod}}$is not motivationally neutral: the neuromodulators that compose it (ACh, NE, 5-HT, DA) are inherently linked to motivational functions (exploration, vigilance, mood/satiety, reward/seeking).

In principle, one could imagine an artificial system with a gain mechanism structurally similar to g_{mod} but not connected to any motivational architecture. Whether such a system would be conscious depends on whether MFS-5 requires only the functional role of the gain mechanism (merely enabling coincidence detection) or also its motivational substrate. This constitutes a "weak" versus "strong" reading of MFS-5 that MSTRT as currently formulated does not resolve.

6.4.9. Verdict

At the conceptual level, consciousness without desire appears conceivable. At the biological level, consciousness without desire appears **practically impossible** in known organisms—the arousal systems that enable consciousness are the same systems that implement basic drives. At the evolutionary level, consciousness without desire would be functionless—an expensive metabolic investment producing no survival benefit.

The unresolved question is whether the apparent inseparability reflects a deep logical necessity or merely a contingent fact about biological evolution. A future artificial system satisfying the formal requirements of MSTRT might achieve consciousness without anything resembling desire. But no naturally occurring system has ever demonstrated this.

6.5. Synthesis: Content Sources vs. Necessary Conditions

6.5.1. The Consistent Pattern

The three domains reveal a consistent pattern. Consciousness has a core mechanism (theta-gamma PAC / BAC firing within a permissive neuromodulatory environment) and a set of content sources that feed into that mechanism. External sensory input, long-term memory, and accumulated knowledge are content sources. They can be absent, impoverished, or substituted without consciousness ceasing.

6.5.2. Two Deep Requirements at the Mechanism–Content Boundary

Two deeper requirements emerge that hover at the boundary between "mechanism" and "content source":

First, ultra-short-term temporal buffering provides the minimum temporal structure without which experience has no duration. This is already captured by MFS-1 and the theta-cycle temporal scaffolding, but this analysis reveals that these specifications implicitly contain a "memory" requirement that should be made explicit.

Second, motivational drive may be so deeply entangled with the biological arousal systems enabling consciousness (MFS-5) that separating them is practically impossible in naturally occurring systems. Whether this is contingent or necessary remains one of the most important open questions in consciousness science.

6.5.3. Implications for MSTRT Architecture

These findings suggest two refinements. MFS-1 should be explicitly annotated to indicate that its temporal integration requirement constitutes a minimal form of memory—unlike episodic, semantic, or working memory—that is likely a necessary condition. MFS-5 should be annotated to indicate that the activation supply is, in all known biological systems, inseparable from motivational drive, and that the question of whether this inseparability is contingent or necessary has direct implications for artificial consciousness.

6.5.4. Summary Table

Evaluation Criterion	MSTRT	IIT	GWT	HOT	DIT	Pred. Coding
Molecular mechanism specification	✓✓✓	✗	✗	✗	✓✓	△
Computable metrics	✓✓✓	△ (NP-hard)	△	✗	✗	△
Anesthesia mechanism explanation	✓✓✓	△	△	✗	✓✓	△
Minimal requirements / specifications	✓✓✓ (6 MFS)	✓ (Φ>o)	△	△	✗	✗
Falsifiable predictions	✓✓✓ (7 preds.)	✓	✓	△	✓	✓
Psychedelic effects explanation	✓✓✓	△	△	✗	✓	✓ (REBUS)
Substrate independence	✓✓ (Process structuralism)	✓✓✓	✓✓	✓✓	△ (Bio-biased)	✓✓
Content domain necessity analysis	✓✓✓	✗	△	✗	✗	△ (Interoception)
Hard problem stance	Does not attempt	✓ (Identity theory)	Does not attempt	△ (Representationalism)	Does not attempt	△ (Controlled hallucination)

✓✓✓ = Comprehensive coverage | ✓✓ = Substantial coverage | ✓ = Partial coverage | △ = Indirect/limited | ✗ = Not covered

Table 1. Systematic comparison of MSTRT with five major theories of consciousness across nine evaluation criteria. The criteria encompass molecular mechanism specification (whether the theory identifies specific molecular/ion channel mechanisms), computable metrics (whether it provides quantitative indices calculable from experimental data), anesthesia mechanism explanation (whether it can explain how general anesthesia abolishes consciousness at the molecular level), minimal requirements/specifications (whether it distills the minimal conditions needed for consciousness), falsifiable predictions (whether it generates specific experimentally refutable predictions), psychedelic effects explanation (whether it can account for psychedelic-induced alterations of consciousness), substrate independence (whether the theory is in principle applicable to non-biological systems), content domain necessity analysis (whether it systematically evaluates whether sensory input/memory/drive are necessary conditions), and hard problem stance (its approach to Chalmers' "hard problem"). MSTRT's principal strengths lie in its comprehensive coverage of molecular mechanism specificity, computable metrics, and systematic content domain analysis. IIT is stronger on substrate independence and hard problem engagement. The six theories are fundamentally complementary rather than opposed.

doi.org/10.32388/YKIRJL

6.6. Implications

6.6.1. Clinical Implications

If external sensory input is not necessary for consciousness, then the failure of a patient to respond to external stimuli cannot be taken as evidence of unconsciousness—a conclusion supported by the discovery of covert consciousness in vegetative state patients[64][65]. If long-term memory is not necessary, then an amnestic patient's inability to recall being conscious does not mean they were not conscious—with direct implications for the ethics of sedation and anesthesia.

The finding that ultra-short-term temporal buffering IS likely necessary provides a potential mechanistic target for distinguishing consciousness from its absence: if theta-gamma PAC and NMDA-dependent temporal integration can be measured (e.g., via PCI or EDRR indices), their absence provides evidence against consciousness in a way that absence of stimulus responsiveness cannot.

6.6.2. Implications for Artificial Consciousness

If the "weak" reading of MFS-5 is correct—that any gain mechanism enabling BAC-equivalent firing suffices, regardless of motivational coloring—then artificial consciousness without desire is possible in principle. If the "strong" reading is correct—that the gain mechanism must be functionally linked to homeostatic/motivational systems—then artificial consciousness would require something functionally analogous to homeostatic drives. The system would need to "care" about something for its information processing to become phenomenally conscious.

6.6.3. Philosophical Implications

The finding that sensory input and long-term memory are not necessary supports the view that consciousness is a mode of processing rather than a type of content. What matters is not what information is being processed but how it is being processed—specifically, whether it is being processed through the nonlinear, multi-scale, temporally structured mechanism that MSTRT identifies. This aligns with the Process Structuralism articulated in Chapter 7.

Chapter 7: Relationship with Other Theories of Consciousness

7.1. Integrated Information Theory (IIT)

Tononi's IIT posits that consciousness is identical to integrated information Φ. IIT's core insight—that consciousness requires information processing that is simultaneously integrated and differentiated—is highly compatible with MSTRT, where global synchronization provides integration and multi-temporal-scale structure provides differentiation. MSTRT is substantially more operationally tractable—every component of $CSDI_{2\cdot0}$ can be computed from electrophysiological data, whereas computing Φ becomes infeasible for systems exceeding ~20 nodes. **Synthesis proposal:** $CSDI_{2\cdot0}$ may be a computable approximation of Φ. IIT's formalism is also compatible with consciousness without desire (a system with high Φ need not have motivational character), placing IIT on the "weak" side of the MFS-5 reading discussed in Chapter 6.

7.2. Global Workspace Theory (GWT)

In MSTRT, GWT's "broadcast" has a precise physical correlate: **the burst firing following BAC firing is the broadcast signal**. The triggering condition is feedforward-feedback coincidence; the carrier is the γ burst; the rhythm is set by the θ cycle. GWT did not specify the physical mechanism of broadcast; MSTRT fills this gap. GWT explicitly allows that the information entering the global workspace can be internally generated—memories, imagined scenarios, spontaneous thoughts—consistent with Chapter 6's finding that external sensory input is not necessary.

7.3. Higher-Order Theory (HOT)

In MSTRT, slow-timescale activity (feedback pathway) "represents" fast-timescale activity (feedforward pathway), and BAC firing is the moment when the two "meet." MSTRT provides a concrete physical implementation for HOT.

7.4. Predictive Coding

Rao and Ballard[66] and Friston[67] developed predictive coding, which maps naturally onto MSTRT: slow oscillations carry "predictions," fast oscillations carry "prediction errors," and PAC represents their systematic coupling. The D_{content}term can be reinterpreted as residual information after compression.

doi.org/10.32388/YKIRJL

7.5. Dendritic Integration Theory (DIT)

Aru, Suzuki, and Larkum[4] proposed that apical dendritic activity in L5 pyramidal neurons is the cellular mechanism of consciousness. MSTRT builds directly upon this foundation. Extensions beyond DIT include: embedding the cellular mechanism within a multi-scale dynamics framework; providing the formal mathematical link from BAC statistics to population-level PAC (Section 2.2.7); constructing computable indices (FRP, EDRR, $CSDI_{2.0}$); distilling substrate-independent MFS; adding the inhibitory interneuron gating framework (Section 2.2.6); and the systematic analysis of content-domain necessity (Chapter 6).

doi.org/10.32388/YKIRJL

7.6. Systematic Comparison

Evaluation Criterion	MSTRT	IIT	GWT	HOT	DIT	Pred. Coding
Molecular mechanism specification	✓✓✓	✗	✗	✗	✓✓	△
Computable metrics	✓✓✓	△ (NP-hard)	△	✗	✗	△
Anesthesia mechanism explanation	✓✓✓	△	△	✗	✓✓	△
Minimal requirements / specifications	**✓✓✓ (6 MFS)**	✓ (Φ>0)	△	△	✗	✗
Falsifiable predictions	**✓✓✓ (7 preds.)**	✓	✓	△	✓	✓
Psychedelic effects explanation	✓✓✓	△	△	✗	✓	✓ (REBUS)
Substrate independence	**✓✓ (Process structuralism)**	✓✓✓	✓✓	✓✓	△ (Bio-biased)	✓✓
Content domain necessity analysis	✓✓✓	✗	△	✗	✗	△ (Interoception)
Hard problem stance	Does not attempt	✓ (Identity theory)	Does not attempt	△ (Representationalism)	Does not attempt	△ (Controlled hallucination)

✓✓✓ = Comprehensive coverage | ✓✓ = Substantial coverage | ✓ = Partial coverage | △ = Indirect/limited | ✗ = Not covered

Table 2. Systematic comparison of MSTRT with five major theories of consciousness across nine evaluation criteria. The criteria encompass molecular mechanism specification (whether the theory identifies specific molecular/ion channel mechanisms), computable metrics (whether it provides quantitative indices calculable from experimental data), anesthesia mechanism explanation (whether it can explain how general anesthesia abolishes consciousness at the molecular level), minimal requirements/specifications (whether it distills the minimal conditions needed for consciousness), falsifiable predictions (whether it generates specific experimentally refutable predictions), psychedelic effects explanation (whether it can account for psychedelic-induced alterations of consciousness), substrate independence (whether the theory is in principle applicable to non-biological systems), content domain necessity analysis (whether it systematically evaluates whether sensory input/memory/drive are necessary conditions), and hard problem stance (its approach to Chalmers' "hard problem"). MSTRT's principal strengths lie in its comprehensive coverage of molecular mechanism specificity, computable metrics, and systematic content domain analysis. IIT is stronger on substrate independence and hard problem engagement. The six theories are fundamentally complementary rather than opposed.

7.7. MSTRT's Philosophical Position — Process Structuralism

The philosophical stance implicit in MSTRT can be termed **Process Structuralism**: consciousness depends on a specific dynamic process structure—not on a specific substrate, nor solely on input-output

doi.org/10.32388/YKIRJL

function, not on specific content (as Chapter 6 demonstrates), but on the spatiotemporal pattern of information flow within the system.

Rejection of substrate dependence: The function of BAC firing does not depend on calcium ions per se, but on the mathematical form of ion channel kinetics, replicable by non-carbon-based systems.

Rejection of pure functionalism: A look-up table can replicate external behavior but internally has no oscillation, no coincidence detection, no recurrence—MSTRT predicts it lacks consciousness.

Rejection of content essentialism: Consciousness does not require specific content types—neither external sensory input, nor memory of the past, nor specific desires. It requires a specific processing architecture operating on some content or other.

Embrace of process structuralism: Any system satisfying the six MFS conditions possesses consciousness, regardless of substrate or content source.

Chapter 8: Testable Experimental Predictions

All predictions below are designed to be falsifiable and do not involve animal experimentation.

Prediction 1: Relationship Between Anesthetic Depth and NLC

Gradually increase anesthetic dosage while recording high-density EEG. Consciousness loss should be marked by a sharp drop in NLC (the nonlinear coupling component), not merely total MI. **Falsification:** If MI and NLC decline simultaneously and proportionally.

Prediction 2: Directional Reversal of CCD

During wakefulness → N2 → N3 sleep, CCD should reverse from positive (top-down) to zero or negative. During REM, CCD should become positive again. **Falsification:** If CCD remains positive across all sleep stages or is negative during REM.

Prediction 3: Emergence of Multi-Scale PAC in Computational Simulation

Simulate the three-layer design (~10,000 spiking neurons). MFS-satisfying networks should spontaneously produce multi-scale PAC; MFS-violating networks should not. **Falsification:** If MFS-violating networks produce equivalent PAC, or MFS-satisfying networks fail to produce PAC.

Prediction 4: EDRR Discrimination in Covert Awareness Patients

Patients clinically diagnosed as vegetative but with covert awareness[64] should have significantly higher EDRR than truly unconscious patients. **Falsification:** If EDRR cannot discriminate between groups.

Prediction 5: Dissociation of NLC and CCD During Psychedelic Experience

Under psilocybin, NLC should increase (more BAC events from lowered threshold) while CCD may remain unchanged or decrease (additional BAC firing driven by noise rather than structured predictions). **Falsification:** If NLC and CCD change in the same direction.

Prediction 6: High Correlation Between $CSDI_{2.0}$ and PCI

$CSDI_{2.0}$ and PCI should be highly positively correlated ($r > 0.8$). **Falsification:** If correlation is below $r = 0.5$.

Prediction 7: Microstate Duration Correlates with Theta Frequency

EEG microstate duration should correlate negatively with dominant cortical theta frequency, and the number of microstates per theta cycle should remain approximately constant (~2–3). **Falsification:** If microstate duration is uncorrelated with theta frequency.

Chapter 9: Discussion and Conclusions

9.1. Principal Contributions

This paper has presented a complete consciousness theory framework spanning from molecular details to system-level dynamics, from structural analysis to dynamic characterization, from necessary conditions to sufficient conditions, and from mechanism specification to content-domain analysis. The principal contributions include:

First, a deep molecular-level explanation of the specificity of consciousness-critical structures—L-type calcium channel kinetics, NMDA receptor Mg^{2+} block, T-type calcium channel oscillation, HCN channel density gradients.

Second, the addition of inhibitory interneuron gating (SST/PV/VIP triad) implementing competitive selection, gamma-phase timing, and attentional gain modulation.

Third, rigorous substitutability analysis yielding a "rigidity-flexibility" spectrum from non-substitutable functions to flexible implementation details.

Fourth, six substrate-independent Minimal Functional Specifications.

Fifth, a complete, computable mathematical framework (FRP, EDRR, $CSDI_{2.0}$) with a formal mathematical link from single-neuron BAC firing statistics to population-level PAC.

Sixth, a general framework for neuromodulation as gain control on consciousness.

Seventh, a systematic empirical evaluation of sensory input, memory, and motivational drive as candidate necessary conditions, establishing that external sensory input and long-term memory are content sources rather than necessary conditions, that ultra-short-term temporal buffering (~200 ms) is very likely necessary and is already embedded in MFS-1/MFS-2, and that motivational drive is practically inseparable from biological arousal mechanisms (MFS-5) even if logically contingent.

Eighth, integration with major existing theories (IIT, GWT, HOT, DIT, predictive coding) and articulation of Process Structuralism.

Ninth, seven falsifiable experimental predictions.

9.2. Limitations

Limitation 1: Multiple parameters in $CSDI_{2.0}$ lack experimental calibration. A specific calibration strategy using well-characterized datasets such as Chennu et al.[68] is proposed.

Limitation 2: The minimal conscious system design is purely theoretical.

Limitation 3: The theory is primarily based on mammalian data. The normalized CSDI (Section 3.5.4) is a first step toward cross-species comparison.

Limitation 4: The "hard problem of consciousness" lies outside the theory's scope.

Limitation 5: The inhibitory interneuron gating framework requires direct experimental testing in the context of consciousness.

Limitation 6: The evidence from hydranencephalic children, while suggestive, remains debated. The meditative states cited as counter-evidence to the necessity of desire rely on first-person reports subject to introspective limitations. The evolutionary entanglement argument applies to biological systems and may not generalize to all possible substrates.

Limitation 7: The distinction between "ultra-short-term temporal buffering" (argued to be necessary) and "working memory" (argued to be non-necessary) rests on a somewhat arbitrary boundary; further empirical work is needed to determine the precise temporal resolution below which consciousness becomes impossible.

9.3. Future Directions

The most urgent next step is to compute $CSDI_{2.0}$ on existing clinical EEG databases and correlate with known consciousness states. The second step is computational simulation of the minimal conscious system design. The third step is neuromorphic hardware implementation. The fourth step is cross-species validation. The fifth step is to design experiments that can empirically test the "weak" versus "strong" reading of MFS-5—potentially by constructing artificial systems that satisfy MFS-1 through MFS-4 and MFS-6 with a gain mechanism that is functionally adequate but not linked to any motivational architecture, and testing whether such systems exhibit consciousness-associated signatures.

9.4. Conclusion

Consciousness resides not in any "magic molecule" or "magic structure," nor in any particular content domain—it is not a mirror of the external world (sensory input is dispensable), not a diary of the past (memory is dispensable), and not necessarily a servant of desire (drives may be contingent). It is, at its core, a specific set of temporal dynamics—the nonlinear nesting and global integration of multi-scale oscillations—that can operate on content from any source, or perhaps on no specific content at all.

Carbon-based biology has evolved elegant molecular machinery to realize these dynamics, and in doing so has deeply entangled the consciousness mechanism with sensory processing, memory systems, and motivational drives. But the analysis presented here suggests that these entanglements are architectural features of the biological implementation rather than logical necessities of consciousness itself. What is necessary is the mechanism: multi-scale temporal resonance, nonlinear coincidence detection, recurrent processing, global integration, sustained activation, and sufficient information capacity—the six Minimal Functional Specifications that any conscious system, biological or artificial, must satisfy.

The value of a theory lies not in whether it is "correct," but in whether it is sufficiently precise and specific that nature can unambiguously tell us whether it is right or wrong. The seven falsifiable predictions of MSTRT are designed precisely for this purpose.

References

1. ^Tononi G (2008). "Consciousness as Integrated Information: A Provisional Manifesto." Biol Bull. **215**(3):216–242.
2. ^Baars BJ (1988). A Cognitive Theory of Consciousness. Cambridge: Cambridge University Press.
3. ^Dehaene S, Sergent C, Changeux JP (2003). "A Neuronal Network Model Linking Subjective Reports and Objective Physiological Data During Conscious Perception." Proc Natl Acad Sci USA. **100**(14):8520–8525.
4. a, b, cAru J, Suzuki M, Larkum ME (2020). "Cellular Mechanisms of Conscious Processing." Trends Cogn Sci. **24**(10):814–825.
5. a, b, cLarkum ME, Zhu JJ, Sakmann B (1999). "A New Cellular Mechanism for Coupling Inputs Arriving at Different Cortical Layers." Nature. **398**(6725):338–341.
6. ^Catterall WA (2011). "Voltage-Gated Calcium Channels." Cold Spring Harb Perspect Biol. **3**(8):a003947.
7. ^Larkum ME, Nevian T, Sandler M, Polsky A, Schiller J (2009). "Synaptic Integration in Tuft Dendrites of Layer 5 Pyramidal Neurons." Science. **325**(5941):756–760.
8. ^Magee JC (1998). "Dendritic Hyperpolarization-Activated Currents Modify the Integrative Properties of Hippocampal CA1 Pyramidal Neurons." J Neurosci. **18**(19):7613–7624.
9. ^Williams SR, Stuart GJ (2000). "Site Independence of EPSP Time Course Is Mediated by Dendritic I_h in Neocortical Pyramidal Neurons." J Neurophysiol. **83**(5):3177–3182.
10. ^Hu W, Tian C, Li T, Yang M, Hou H, Shu Y (2009). "Distinct Contributions of Nav1.6 and Nav1.2 in Action Potential Initiation and Backpropagation." Nat Neurosci. **12**:996–1002.
11. ^Stuart GJ, Sakmann B (1994). "Active Propagation of Somatic Action Potentials Into Neocortical Pyramidal Cell Dendrites." Nature. **367**(6458):69–72.
12. a, bSuzuki M, Larkum ME (2020). "General Anesthesia Decouples Cortical Pyramidal Neurons." Cell. **180**(4):666–676.
13. ^González-Maeso J, Weisstaub NV, Zhou M, et al. (2007). "Hallucinogens Recruit Specific Cortical 5-HT2A Receptor-Mediated Signaling Pathways." Neuron. **53**(3):439–452.
14. ^Muñoz W, Tremblay R, Levenstein D, Bhatt DK, Rudy B (2017). "Layer-Specific Modulation of Neocortical Dendritic Inhibition During Active Wakefulness." Science. **355**(6328):954–959.
15. ^Cardin JA, Carlén M, Meletis K, et al. (2009). "Driving Fast-Spiking Cells Induces Gamma Rhythm and Controls Sensory Responses." Nature. **459**(7247):663–667.

16. ^ Huguenard JR, McCormick DA (1992). "Simulation of the Currents Involved in Rhythmic Oscillations in Thalamic Relay Neurons." J Neurophysiol. **68**(4):1373–1383.

17. ^ Destexhe A, McCormick DA, Sejnowski TJ (1993). "A Model for 8–10 Hz Spindling in Interconnected Thalamic Relay and Reticularis Neurons." Biophys J. **65**(6):2473–2477.

18. ^ Landisman CE, Long MA, Beierlein M, Deans MR, Paul DL, Connors BW (2002). "Electrical Synapses in the Thalamic Reticular Nucleus." J Neurosci. **22**(3):1002–1009.

19. ^ Steriade M, McCormick DA, Sejnowski TJ (1993). "Thalamocortical Oscillations in the Sleeping and Aroused Brain." Science. **262**(5134):679–685.

20. ^ Crick FC (1984). "Function of the Thalamic Reticular Complex: The Searchlight Hypothesis." Proc Natl Acad Sci USA. **81**(14):4586–4590.

21. ^ McAlonan K, Cavanaugh J, Wurtz RH (2008). "Guarding the Gateway to Cortex with Attention in Visual Thalamus." Nature. **456**(7220):391–394.

22. ^ Llinás R, Ribary U (1993). "Coherent 40-Hz Oscillation Characterizes Dream State in Humans." Proc Natl Acad Sci USA. **90**(5):2078–2081.

23. ^ Covic EN, Sherman SM (2011). "Synaptic Properties of Connections Between the Primary and Secondary Auditory Cortices in Mice." Cereb Cortex. **21**(11):2425–2441.

24. ^ De Pasquale R, Sherman SM (2011). "Synaptic Properties of Corticocortical Connections Between the Primary and Secondary Visual Cortical Areas in the Mouse." J Neurosci. **31**(46):16494–16506.

25. ^ Mayer ML, Westbrook GL, Guthrie PB (1984). "Voltage-Dependent Block by Mg^{2+} of NMDA Responses in Spinal Cord Neurones." Nature. **309**(5965):261–263.

26. ^ Nowak L, Bregestovski P, Ascher P, Herbet A, Prochiantz A (1984). "Magnesium Gates Glutamate-Activated Channels in Mouse Central Neurones." Nature. **307**(5950):462–465.

27. ^ a, b Wang XJ (2001). "Synaptic Reverberation Underlying Mnemonic Persistent Activity." Trends Neurosci. **24**(8):455–463.

28. ^ Crick FC, Koch C (2005). "What Is the Function of the Claustrum?" Philos Trans R Soc Lond B. **360**(1458):1271–1279.

29. ^ Wang Q, Ng L, Harris JA, et al. (2017). "Organization of the Connections Between Claustrum and Cortex in the Mouse." J Comp Neurol. **525**(6):1317–1346.

30. ^ Anastassiou CA, Perin R, Markram H, Koch C (2011). "Ephaptic Coupling of Cortical Neurons." Nat Neurosci. **14**(2):217–223.

31. ^Penrose R (1994). Shadows of the Mind. Oxford: Oxford University Press.

32. ^Hameroff S, Penrose R (2014). "Consciousness in the Universe: A Review of the 'Orch OR' Theory." Phys Life Rev. **11**(1):39–78.

33. ^Tegmark M (2000). "Importance of Quantum Decoherence in Brain Processes." Phys Rev E. **61**(4 Pt B):4194–4206.

34. ^Engel GS, Calhoun TR, Read EL, et al. (2007). "Evidence for Wavelike Energy Transfer Through Quantum Coherence in Photosynthetic Systems." Nature. **446**(7137):782–786.

35. ^Fisher MPA (2015). "Quantum Cognition: The Possibility of Processing with Nuclear Spins in the Brain." Ann Phys. **362**:593–602.

36. ^Bassett DS, Bullmore E (2006). "Small-World Brain Networks." Neuroscientist. **12**(6):512–523.

37. ^Tort ABL, Komorowski R, Eichenbaum H, Kopell N (2010). "Measuring Phase-Amplitude Coupling Between Neuronal Oscillations of Different Frequencies." J Neurophysiol. **104**(2):1195–1210.

38. a, bNieder A, Wagener L, Rinnert P (2020). "A Neural Correlate of Sensory Consciousness in a Corvid Bird." Science. **369**(6511):1626–1629.

39. ^VanRullen R, Koch C (2003). "Is Perception Discrete or Continuous?" Trends Cogn Sci. **7**(5):207–213.

40. ^Lehmann D, Strik WK, Henggeler B, König T, Koukkou M (1998). "Brain Electric Microstates and Momentary Conscious Mind States." Int J Psychophysiol. **29**(1):1–11.

41. ^Llinás R, Paré D (1991). "Of Dreaming and Wakefulness." Neuroscience. **44**(3):521–535.

42. ^Cole J (1995). Pride and a Daily Marathon. Cambridge: MIT Press.

43. ^Weiskrantz L (1986). Blindsight: A Case Study and Implications. Oxford: Oxford University Press.

44. ^Corkin S (2013). Permanent Present Tense. New York: Basic Books.

45. ^DeCasper AJ, Fifer WP (1980). "Of Human Bonding: Newborns Prefer Their Mothers' Voices." Science. **208**(4448):1174–1176.

46. ^Baars BJ, Franklin S (2003). "How Conscious Experience and Working Memory Interact." Trends Cogn Sci. **7**(4):166–172.

47. ^Lavie N (2005). "Distracted and Confused?: Selective Attention Under Load." Trends Cogn Sci. **9**(2):75–82.

48. ^Dehaene S, Naccache L (2001). "Towards a Cognitive Neuroscience of Consciousness." Cognition. **79**(1–2):1–37.

49. ^James W (1890). The Principles of Psychology. New York: Henry Holt and Company.

50. ^Wang XJ (1999). "Synaptic Basis of Cortical Persistent Activity: The Importance of NMDA Receptors to Working Memory." J Neurosci. **19**(21):9587–9603.

51. ^Pöppel E (1997). "A Hierarchical Model of Temporal Perception." Trends Cogn Sci. **1**(2):56–61.

52. ^Raymond JE, Shapiro KL, Arnell KM (1992). "Temporary Suppression of Visual Processing in an RSVP Task: An Attentional Blink?" J Exp Psychol Hum Percept Perform. **18**(3):849–860.

53. ^Sergent C, Dehaene S (2004). "Is Consciousness a Gradual Phenomenon?" Psychol Sci. **15**(11):720–728.

54. ^Panksepp J (1998). Affective Neuroscience: The Foundations of Human and Animal Emotions. New York: Oxford University Press.

55. ^Solms M (2021). The Hidden Spring: A Journey to the Source of Consciousness. New York: W.W. Norton.

56. ^Merker B (2007). "Consciousness Without a Cerebral Cortex: A Challenge for Neuroscience and Medicine." Behav Brain Sci. **30**(1):63–81.

57. ^Damasio A (1994). Descartes' Error. New York: Putnam.

58. ^Damasio A (1999). The Feeling of What Happens. New York: Harcourt Brace.

59. ^Damasio A (2010). Self Comes to Mind. New York: Pantheon.

60. ^Seth AK, Tsakiris M (2018). "Being a Beast Machine: The Somatic Basis of Selfhood." Trends Cogn Sci. **22**(11):969–981.

61. ^Craig AD (2009). "How Do You Feel—Now? The Anterior Insula and Human Awareness." Nat Rev Neurosci. **10**(1):59–70.

62. ^Josipovic Z (2014). "Neural Correlates of Nondual Awareness in Meditation." Ann NY Acad Sci. **1307**(1):9–18.

63. ^Moruzzi G, Magoun HW (1949). "Brain Stem Reticular Formation and Activation of the EEG." Electroencephalogr Clin Neurophysiol. **1**(1–4):455–473.

64. a, bOwen AM, Coleman MR, Boly M, Davis MH, Laureys S, Pickard JD (2006). "Detecting Awareness in the Vegetative State." Science. **313**(5792):1402.

65. ^Monti MM, Vanhaudenhuyse A, Coleman MR, et al. (2010). "Willful Modulation of Brain Activity in Disorders of Consciousness." N Engl J Med. **362**(7):579–589.

66. ^Rao RPN, Ballard DH (1999). "Predictive Coding in the Visual Cortex." Nat Neurosci. **2**:79–87.

67. ^Friston K (2010). "The Free-Energy Principle: A Unified Brain Theory?" Nat Rev Neurosci. **11**(2):127–138.

68. ^Chennu S, Finoia P, Kamau E, et al. (2014). "Spectral and Connectivity Markers of Consciousness." PLoS Comput Biol. **10**(10):e1003887.

Declarations

Funding: No specific funding was received for this work.

Potential competing interests: No potential competing interests to declare.